

University of Nebraska - Lincoln

## DigitalCommons@University of Nebraska - Lincoln

---

Dissertations and Theses in Biological Sciences

Biological Sciences, School of

---

Winter 12-7-2010

# Study Of Two Human Myotubularin Homologs (AtMTM1 and AtMTM2) In Arabidopsis

Yang Zhao

University of Nebraska - Lincoln, zhao.yang.fudan@gmail.com

Follow this and additional works at: <https://digitalcommons.unl.edu/bioscidiss>



Part of the [Life Sciences Commons](#), and the [Medicine and Health Sciences Commons](#)

---

Zhao, Yang, "Study Of Two Human Myotubularin Homologs (AtMTM1 and AtMTM2) In Arabidopsis"

(2010). *Dissertations and Theses in Biological Sciences*. 21.

<https://digitalcommons.unl.edu/bioscidiss/21>

This Article is brought to you for free and open access by the Biological Sciences, School of at DigitalCommons@University of Nebraska - Lincoln. It has been accepted for inclusion in Dissertations and Theses in Biological Sciences by an authorized administrator of DigitalCommons@University of Nebraska - Lincoln.

STUDY OF TWO HUMAN MYOTUBULARIN HOMOLOGS (AtMTM1 AND  
AtMTM2) IN *ARABIDOPSIS*

by

Yang Zhao

A THESIS

Presented to the Faculty of  
The graduate College at the University of Nebraska  
In partial Fulfillment of Requirements  
For the Degree of Master of Science

Major: Biological Sciences  
Under the Supervision of Professor Zoya Avramova

Lincoln, NE

December, 2010

STUDY OF TWO HUMAN MYOTUBULARIN HOMOLOGS (AtMTM1 AND  
AtMTM2) IN *ARABIDOPSIS*

Yang Zhao, MS

University of Nebraska, 2010

Advisor: Zoya Avramova

Phosphatidylinositol 5 phosphate is appearing to play an important role in signal transduction as lipid second messenger. The synthesis of this lipid signal is mainly conducted by a group of phosphatase called myotubularins (MTM) which can dephosphorylate on the 3's position of Phosphatidylinositol (3, 5) bi-phosphate. Mutations in active myotubularins lead to severe diseases in human. However, this essential family has been scarcely studied in plants. Recently, two myotubularins (AtMTM1 and AtMTM2) have been identified as the homologs of human MTM Related protein 2 (MTMR2) in *Arabidopsis*. While some evidence has been provided to suggest the function of AtMTM1, the knowledge of AtMTM2 is really little. In this study, we reported here that AtMTM1 increases significantly in hydathods after dehydration stress but no obvious change on AtMTM2 expression was observed, while both extensively present in roots, leaves, flowers and siliques. AtMTM2 exists not only in cytoplasm and membrane like AtMTM1, but also in the nucleus. *AtMTM1* knockout mutant showed a more tolerant phenotype to drought compared with wild type, but knockout of *AtMTM2* didn't cause visible deviation. Obtained results provide a ground for comprehensive further studies of AtMTM2 function and comparisons with AtMTM1.

**TABLE OF CONTENTS**

ACKNOWLEDGMENTS .....	2
GOALS OF MY STUDY .....	3
INTRODUCTION .....	4
RESULTS.....	14
GUS Expression Analysis of <i>AtMTM1</i> and <i>AtMTM2</i> gene .....	14
mRNA level of AtMTM1 and AtMTM2 in different tissues .....	19
The subcellular localization of AtMTM1 and AtMTM2 .....	21
Selection of <i>AtMTM1</i> and <i>AtMTM2</i> mutants .....	23
Phenotypic Analysis.....	32
MATERIALS AND METHODS .....	35
1.GUS Expression Analysis .....	35
2.Dehydration Stress Treatment.....	38
3.Determination of mRNA Levels by qRT-PCR.....	38
4.Transient Expression of AtMTM1 and AtMTM2 in Tobacco Leaves .....	40
5.Selection for Mutants and Phenotype Screens.....	42
6.Generating Double Mutants for <i>atmtm1/atmtm2</i> .....	45
DISCUSSION .....	46
Tissue specific expression of <i>AtMTM1</i> and <i>AtMTM2</i> in <i>Arabidopsis</i> .....	46
Quantitative test of <i>AtMTM1</i> and <i>AtMTM2</i> after dehydration .....	47
Cytoplasmic AtMTM1 but nuclear AtMTM2? .....	48
Phenotypic characterization of mutant plants .....	49
CONCLUSION.....	51
REFERENCED LITERATURE.....	52

## ACKNOWLEDGMENTS

I would like to sincerely thank my advisor Dr. Zoya Avramova for the research opportunity and her support during these three years. I have learnt a lot under her guidance both in academic career and in real life. I wish to also express my thanks to my committee members: Dr. John Osterman, who inspired me about the elegance of genetics and helped with my teaching, and Dr. Joseph A. Turner, for turning my attention to a different, but nonetheless exciting, area of cell biology. My gratitude extends to my colleagues in the laboratory: Ivan Ndamukong, Hanna Lapko and Yong Ding, who taught me a lot in experimental techniques. I learnt more than I ever expected. Also, I owe thanks to the Green House and the Microscope facility staff: I bothered them almost every week during my Master's program.

Without the help of all these people, I would have not been able to complete this program.

## GOALS OF MY STUDY

- 1) to define the tissue specific expression of *AtMTM1* and *AtMTM2*, and the change upon dehydration stress, as a step to understanding their function and relationship.
- 2) to investigate AtMTM1 and AtMTM2 subcellular localization and to find out whether they can interact and dimerize.
- 3) to isolate *AtMTM1* and *AtMTM2* *Arabidopsis* mutants, and to compare phenotypes between them in drought condition; a phenotype could suggest function.

## INTRODUCTION

Phosphatidylinositol (PtdIns) is a class of phospholipids composed of glycerol, a fatty acid chain, and a hexahydric alcohol (inositol), which distributes in the bilayer-membrane of all eukaryotic cells. Although not as abundant as phosphatidylcholine, phosphatidylethanolamine and phosphatidylserine, the PtdIns are important ligands in cellular signaling process. Phosphate group can be added to the inositol ring head, hexahydroxycyclohexane, on the position 3, 4 and/or 5 (**Figure 1**), which may form 7 different phosphoinositides (Tolias and Cantley 1999). These phospholipids are involved in a variety of cellular processes, including calcium regulation, vesicle trafficking, endocytosis regulation, signal transduction that regulates cell survival and mitogenesis, and cellular compartmentalization through actin rearrangement (Tolias and Cantley 1999; De Matteis and Godi 2004; Lorenzo, Urbe et al. 2006). PtdIns function not only as precursors of second messengers. They also can directly recruit specific signaling proteins to the membrane.

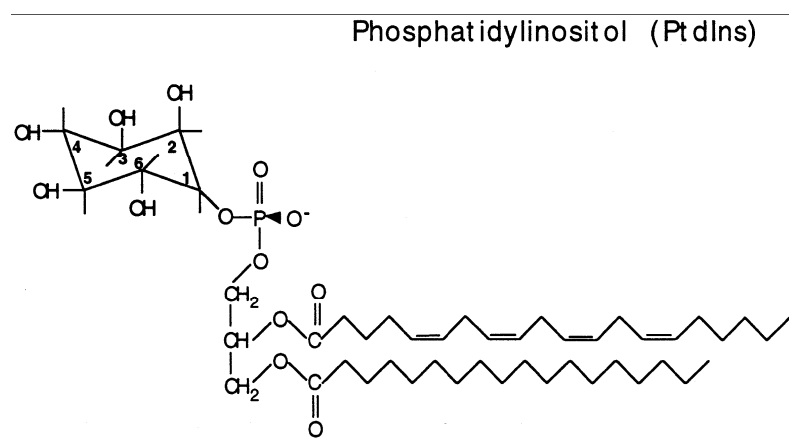


**Figure 1:** Chemical structure of PtdIns (Tolias and Cantley 1999).

Among the 7 phosphoinositides, three phosphatidylinositol monophosphates, PtdIns(3)P, (PI3P), PtdIns(4)P, (PI4P), and PtdIns(5)P,(PI5P), are emerging as major players in cellular signaling and trafficking (Pendares, Tronchere et al. 2005). PI3P is constitutively present, at a constant level, in mammalian cells and is located mainly

on intravesicular membranes. It functions as a spatial regulator in vesicular trafficking by interacting with a number of proteins involved in the process. For example, PI3P can bind PX domain in trafficking process (Ponting 1996) as well as a set of FYVE domain-containing proteins involved in vacuolar sorting (Gaullier, Simonsen et al. 1998). By comparison, PI4P is associated mainly with the Golgi complex. PI4P is most abundant in the Golgi at steady state in mammalian cells (Wang, Wang et al. 2003; De Matteis and Godi 2004). As a signature feature establishing the unique organelle identity, PI4P recruits Golgi-associated proteins such as epsinR, oxysterol binding protein, the clathrin adaptor AP-1 and the fourphosphate-adaptor protein 1 & 2 to the Golgi complex (Levine and Munro 2002; Hirst, Motley et al. 2003; Wang, Wang et al. 2003). PI4P is involved also in diverse cell functions such as regulating early steps of phagocytosis (Godi, Di Campli et al. 2004), the control of stomatal movements in plants (Jung, Kim et al. 2002), and the regulation of neuronal Cl<sup>-</sup> ATPaseXpump in animal cells (Wu, Kitagawa et al. 2002). The detailed functions of PI4P in those processes, at the molecular level, are still unclear.

PI5P is the least characterized and is present in the lowest amount among all of them (1–5% of the total PtdInsP). Historically, it has been ignored but after its identification as the substrate for the known messenger, phosphatidylinositol (4,5)-bisphosphate, PtdIns(4,5)P<sub>2</sub> in mammalian fibroblasts (Rameh, Tolias et al. 1997), studies of PI5P have rocketed (Lecompte, Poch et al. 2008). PI5P is emerging as a major component (ligand) in signal transduction pathways regulating a broad variety of cellular functions. Deregulation of PI5P homeostasis is associated with severe human diseases (Pendaries, Tronchere et al. 2005). The diverse functions of PI5P include membrane trafficking, mainly the regulation of membrane transport from late endosomal compartments to the plasma membrane, participation in immune response

during cell invasion by the human intestinal pathogen *Shigella flexneri*, control of cell morphology and actin assembly and, recently, nuclear signaling (Niebuhr, Giuriato et al. 2002; Sbrissa, Ikonomov et al. 2004; Pendaries, Tronchere et al. 2005).

The level of endogenous PI5P is not constant. It is very low in resting cells, but high upon thrombin stimulation in human platelets (Morris, Hinchliffe et al. 2000) or under stress conditions such as osmotic stress in mammalian and in yeast cells (Meijer, Berrie et al. 2001; Sbrissa, Ikonomov et al. 2002). It also increases by 20-fold during the G1 phase unraveling a potential role for PtdIns(5)P in cell-cycle progression (Clarke 2003). Since signaling by lipids in the nucleus is still poorly known, it was unexpected to find PI5P as a second messenger in the nucleus (Gozani, Karuman et al. 2003). The observation that PI5P can bind to the plant homeodomain (PHD) of inhibitor of growth protein 2 (ING2), a conserved Cys4-HisCys3 zinc finger suggested involvement in a signaling mechanism (Gozani, Karuman et al. 2003). ING2 is a candidate tumor suppressor that induces growth arrest and apoptosis in a p53-dependent manner (Pendaries, Tronchere et al. 2005). Through their interaction, PI5P affects both the distribution and the activity of ING2. It regulates the functions of ING proteins by either, (a) retaining ING2 within the nucleus; (b) enhancing protein-protein interactions with nuclear factors; or (c) stimulating or inhibiting ING-associated chromatin modifying activities (Bua and Binda 2009). Loss of this interaction caused a decrease in ING2- mediated apoptosis and p53 acetylation affecting, thus, the cell cycle progression. Binding to other chromatin remodeling proteins, PI5P plays an important role in regulating changes in chromatin structure to modulate gene expression, replication, DNA repair or RNA splicing(Clarke 2003; Jones and D. 2004; Gozani, Field et al. 2005; Bunce, Gonzales et al. 2006). The PHD domain found in the epigenetic factor, ATX1, the *Arabidopsis* Trihorax-like protein

also binds specifically PI5P and affects the regulation of genes controlled by ATX1 (Alvarez-Venegas 2006).

However, existence of PI5P has not been positively identified in *Arabidopsis*. Because it is hard to separate from PI4P by high performance liquid chromatography (HPLC), and PI4P cellular level is much more abundant than putative PI5P level. Recently, Ndamukong et al radioactively labeled the 4' position of PI5P and PI3P with PI4K $\alpha$ , and then separated the PI(4,5)P<sub>2</sub> from PI(3,4)P<sub>2</sub> by HPLC. Thus, they firstly identified PI5P in *Arabidopsis* and determined its level in rosette leaves, stems, inflorescences, and siliques (Ndamukong, Jones et al. 2010). Importantly, PI5P levels significantly increased under dehydration stress(Ndamukong, Jones et al. 2010). This change in PtdIns5P was shown to negatively influence the activity of ATX1 at the promoter region of ATX1 dependent genes, such as *WRKY70*. This negative effect on ATX1 activity was due to the relocation of ATX1 from the nucleus into the cytoplasm. Decreased presence of ATX1 at the *WRKY70* locus was reflected by lower level of Histone 3 Lysine 4 tri-methylation (H3K4me3) accumulation, a chromatin marker for an active state, and lower expression levels of the *WRKY70* gene. Thus, PI5P establishes a link between chromatin modification and endogenous lipid-levels. Since PI5P concentrations increase upon dehydration stress (Ndamukong et al., 2010), it is crucial to understand its metabolism. PI5P can be produced from 3 sources (**Figure 2**): PI, PI(4,5)P<sub>2</sub> and PI(3,5)P<sub>2</sub>. Phosphorylation of PI via a 5-kinase(PIKfyve) can form PI5P (Shisheva 2001; Sbrissa, Ikonomov et al. 2002) but existence of such kinases is still debatable. Current evidence suggests that PI5P is generated from the dephosphorylation of PtdIns(3,5)P<sub>2</sub> or PtdIns(4,5)P<sub>2</sub> (Lecompte, Poch et al. 2008).

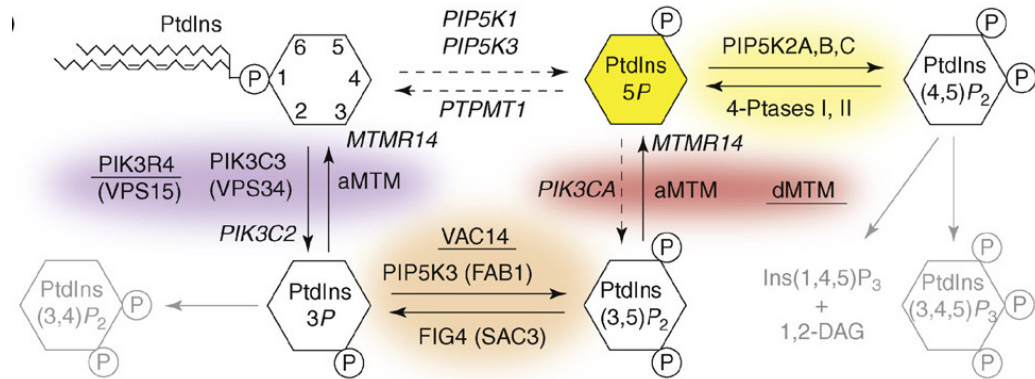


**Figure 2:** putative metabolic pathways of PI5P synthesis and transformation. Fatty acids are represented for PtdIns only. Proteins that are putatively implicated in PtdIns5P turnover are indicated according to the experimental evidence supporting their role: in vivo data is shown in black, and in vitro data is shown in italics. Broken arrows indicate putative phosphoinositide transformation. Known and potential regulators are underlined (Lecompte, Poch et al. 2008).

The myotubularins are phosphatases that convert PtdIns(3,5)P<sub>2</sub> to PI5P (Walker, Urbe et al. 2001; Tronchere, Buj-Bello et al. 2003; Tronchere, Laporte et al. 2004). Each of the Myotubularin (MTM) family members contains a putative PH-GRAM (Pleckstrin Homology-Glucosyl transferases, Rab-like GTPase activators and myotubularins) domain, a coiled-coil region, and a the catalytic phosphatase domain (Clague and Lorenzo 2005) (**Figure 3**). In human, there are 14 MTM family members , eight of which maintain enzymatically active protein tyrosine phosphatase (PTP) domain. These active (aMTM) proteins are MTM1, myotubularin- related 1 (MTMR1), MTMR2, MTMR3, MTMR4, MTMR6, MTMR7 and MTMR8. The other 6 myotubularins (dMTM) have mutated sequences at the active site and, consequently, are inactive as phosphatases (Clague and Lorenzo 2005). Nonetheless, the nonactive myotubularins have been conserved during evolution suggesting important, albeit unclear, cellular functions.

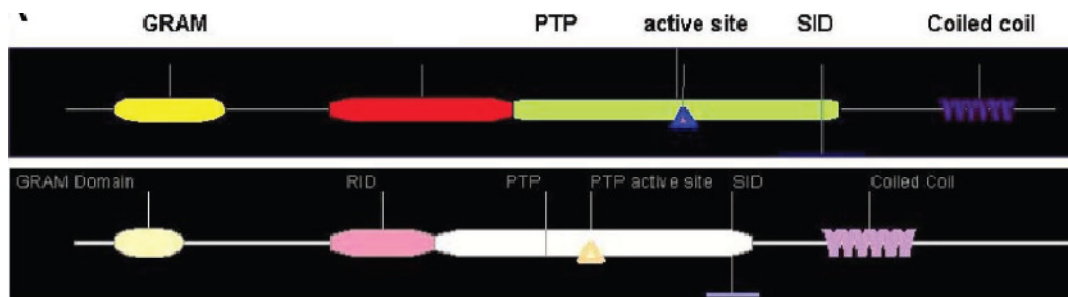


**Figure 3:** Structure of the human MTMR2 (top) and the *Arabidopsis* At3g10550 protein AtMTM (bottom) (Ding, Lapko et al. 2009). Domains are as defined in Begley and Dixon (Begley and Dixon 2005)

The catalytically active myotubularins specifically target the 3' position on the phosphatidylinositol head group. They can dephosphorylate PI3P and PtdIns(3,5)P<sub>2</sub>, to generate PtdIns and PtdIns(5)P, respectively. It is known that loss of function of MTM1 causes myotubular myopathy, a pathology characterized by the malformation of skeletal muscle myotubes (Laporte, Hu et al. 1996). Defect of MTMR2 and MTMR13 also lead to Charcot-Marie-Tooth neuropathy (Bolino, Muglia et al. 2000; Azzedine, Bolino et al. 2003), and mutation of MTMR2 and MTMR5 lead to impaired spermatogenesis (Bua and Binda 2009).

The process of PI5P generation by MTM involves the class-III PtdIns 3-kinases (PIK3C3) and the type-III phosphatidylinositol-3-phosphate 5-kinase. After being produced by PIK3C3, PI3P is then phosphorylated to PtdIns(3,5)P<sub>2</sub> by the kinase, PIP5K3. This bi-phosphate serves as a substrate for the aMTM phosphatase activities, which, by removing the phosphate at 3' position produce the monophosphate PtdIns5P (Pendaries, Tronchere et al. 2006). Based on this pathway, and some evidence of phosphoinositide-3-kinase regulatory subunit 4(PIK3R4), it was proposed that the substrate specificity of aMTM is determined by a larger complex which integrates an aMTM (Cao, Laporte et al. 2007; Lecompte, Poch et al. 2008). In the a ternary PIK3R4–PIK3C3– aMTM complex, PIK3R4 regulates the sequential production and degradation of PtdIns3P on endosomes where aMTM preferentially

dephosphorylates PtdIns3P rather than PtdIns(3,5)P<sub>2</sub>. But in another complex, PIK3C–dMTM–aMTM, aMTM can form heterodimers with dMTM. At least 4 pairs of the heterodimers have been reported, such as dMTMR13–aMTMR2 heterodimers (Robinson and Dixon 2005; Berger, Berger et al. 2006; Lorenzo, Urbe et al. 2006). Heterodimerized aMTM in such a context would specifically dephosphorylate PtdIns(3,5)P<sub>2</sub>.

MTMs are mostly cytoplasmic proteins. However, it is hotly debated whether some MTM members or isoforms can enter the nucleus to produce a functional nuclear phospholipid signal. MTMs have no nuclear localization signal (NLS). However, about 40% of the nuclear proteins do not carry a detectable NLS. Furthermore, a domain that specifically binds to the SET domain of Trithorax proteins (ATX1 is a member of this family) is conserved in all MTM family members. This SET-binding domain (SID) (see Figure 3) may promote an interaction with nuclear (chromatin) factors. However, studies of the 3D structure of MTM has revealed that the SET binding domain is largely located within the catalytically active region, it was suggested that this domain is required for the structural integrity rather than interacting with SET domain *in vivo* (Clague and Lorenzo 2005). More studies are required to establish the physiological significance of the MTM binding to the trithorax SET and a potential role in the nucleus. Lastly, the evidence that MTMR2 and MTMR5 co-localize at the nuclear periphery (Kim, Vacratsis et al. 2003), suggests that these two enzymes may generate PI5P functioning in the nucleus.

In *Arabidopsis*, there only two genes PI5P MTM pathway may also exist. Two homologs of human MTMR2 were found. They are named AtMTM1 and AtMTM2, and encoded by *Arabidopsis* gene, *At3g10550* and *At5g 04540* respectively. AtMTM1 and AtMTM2 are 77% identical while sharing 85% similarity. And with

human MTMR2, they are 38% identical with 59% similarity (**Figure 3**). Furthermore, both of the two plant homologs are conserved in those consensus amino acids critical for enzyme activity of the human aMTM (Ding, Lapko et al. 2009).

Compared with the wealth of knowledge of their counterpart in human, MTMR2, AtMTM1 and AtMTM2 are poorly studied. So far, data has shown that AtMTM1 is actively evolved in PI5P metabolism in *Arabidopsis* (Ding, Lapko et al. 2009; Ndamukong, Jones et al. 2010). Ding et al first measured the phosphatase activity of AtMTM1 in vitro. They showed AtMTM1 prefers PI(3,5)P<sub>2</sub> as substrate (the Km and Vmax of AtMTM1 is 146 μM and 0.12 nmol/min/mg for PI(3)P, contrasted by 101μM and 0.16 nmol/min/mg for PI(3,5)P<sub>2</sub>). They also claimed the expression of AtMTM1 sharply increases under osmosis stress. But they didn't provide any evidence that PI5P level increases in the same condition. In addition, by microarray assays, they discovered AtMTM1 regulates a common set of genes with ATX1 under dehydration condition. 140 genes are altered after stress is introduced in both AtMTM1 over expressed mutant and ATX1 knockout mutant, 106 of which are significantly down regulated. Therefore, the *AtMTM1* and *ATX1* mutants present similar phenotype compared with wild type Columbia 0, especially in the response to dehydration and re-hydration.

Then in 2010, Ndamukong et al proved PI5P level is indeed increased after drought stress in *Arabidopsis*, which suggests the AtMTM1 phosphatase activity *in vivo* combined with Ding et al data. Besides *AtMTM1* overexpress mutant, they also investigated the knockout mutant. And they found the PI5P level is higher in overexpress mutant but lower in the knockout mutant than wild type in both normal and stress condition. Thus, it is confirmed that AtMTM1 is responsible for PI5P production. Moreover, they demonstrated AtMTM1 regulates the distribution of ATX1.

This re-localization of ATX1 requires both functional PTP domain in AtMTM1 and PHD domain in ATX1, which indicates the real regulator is PI5P instead of the direct interaction between the two proteins. Finally, but more importantly, they proved the re-distribution of ATX1 can lead to change of the H3K4 trimethylation marker, and therefore affect downstream gene expressions, such as WRKY 70.

All together, current evidence has indicated a epigenetic pathway linking environment stress to gene expression in *Arabidopsis*. The osmosis stress causes an increase of AtMTM1, which then elevates the level of lipid signal PI5P. PI5P relocates ATX1 into cytoplasm from the nucleus by binding its PHD domain. Leaving from nucleus leads to significant decrease of ATX1 methylation activity on the chromatin. Since the H3K4 trimethylation is an active epigenetic marker, a large number of ATX1 dependent genes would be affected.

However, current the pathway mechanism doesn't account the AtMTM2, which is closely related to AtMTM1. We propose two hypothesis about AtMTM2 function: the first one is that based on their similarities, AtMTM2 might be redundant to AtMTM1. When they are both expressed, the effect of either one can be compensated by the other. Or they probably have different tissue specificity. In this case, AtMTM1 can specifically regulates the PI5P in some organs like leaves, whereas AtMTM2 prefers to exert phosphatase function in other parts like roots.

The other hypothesis is based the character of human MTMR2. Early studies showed MTMR2 can self-dimerize and heterodimerize with 3 dMTMs: MTMR5, MTMR12 as well as MTMR13 by the interaction between their coiled-coil domains. And the heterodimerization can greatly increase the activity of MTMR2, for example: MTMR2 activity increases to 3 to 4 fold after addition of MTMR5 in vitro. Furthermore, mutations in either of MTMR2 or MTMR5 lead to defective

spermatogenesis (Firestein, Nagy et al. 2002; Bolino, Bolis et al. 2004). Similarly, mutations in either MTMR2 or MTMR13 leads to clinically indistinguishable forms of Charcot–Marie–Tooth syndrome also confirms the physiological significance of formation of heterodimer (Robinson and Dixon 2005). Besides activity, the specificity can be regulated by the dMTM, too (Lecompte, Poch et al. 2008). In the case that aMTM interacts with dMTM, aMTM has a higher activity to PI(3,5)P<sub>2</sub>. But without dMTM, it prefers PI3P rather than PI(3,5)P<sub>2</sub>. Thus, it is logical to hypothesize AtMTM2 may play a similar regulatory role to AtMTM1 if AtMTM2 is inactive.

Unfortunately, AtMTM2 has been never studied. Therefore, in this thesis we will compare the expression profile of AtMTM1 and AtMTM2, investigate their subcellular localization and interaction, and observe the knockout mutant phenotype of each one as well as double mutant. The result of this study will provide some clue for understanding the relationship between AtMTM1 and AtMTM2.

## RESULTS

### GUS Expression Analysis of *AtMTM1* and *AtMTM2* gene

The expression patterns of proteins always suggest their functions. So we first studied where the *AtMTM1* and *AtMTM2* exist. To investigate the tissue-specificity of *AtMTM1* and *AtMTM2* expression, we generated transgenic *Arabidopsis* lines which stably expressed the GUS under the control of *AtMTM1* and *AtMTM2* promoter, respectively. We used pCambia 1303 vector to express the *GUS* gene. In the original vector, *GUS* is controlled by the 35S promoter which would be replaced by *AtMTM1* or *AtMTM2* promoter in transgenic lines (Figure 4).

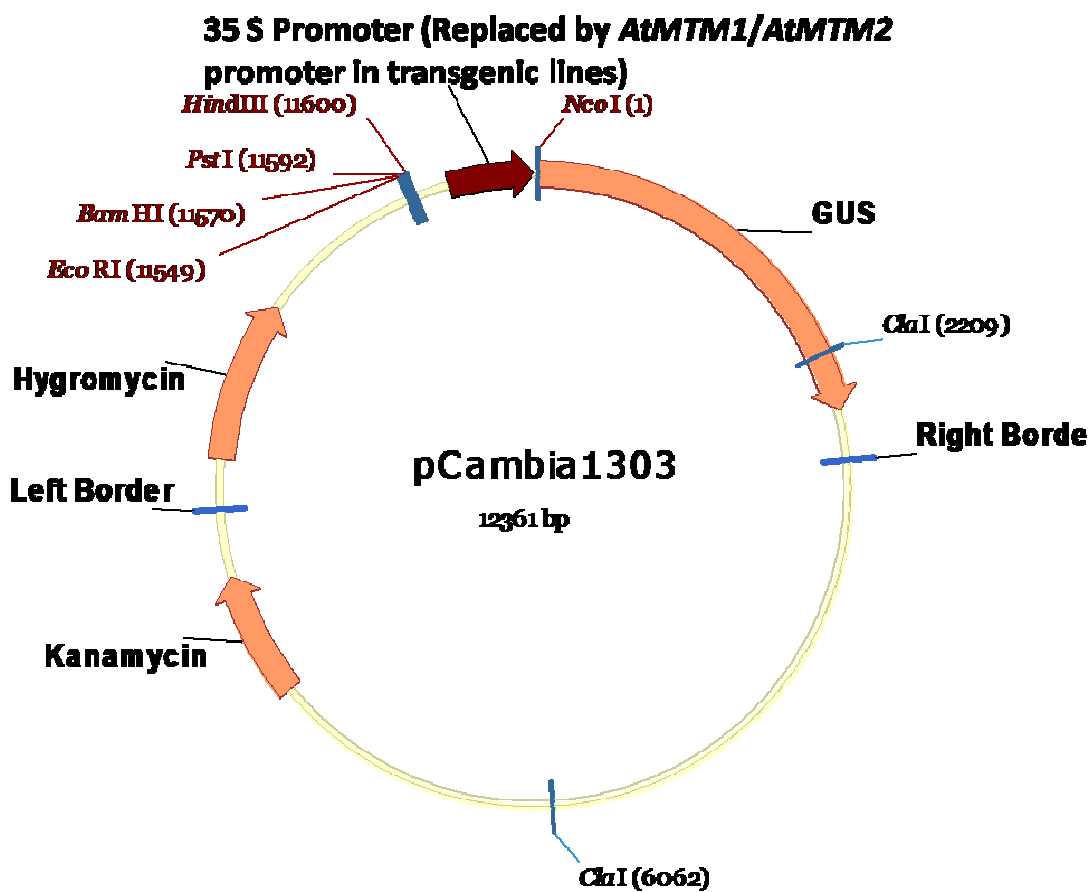
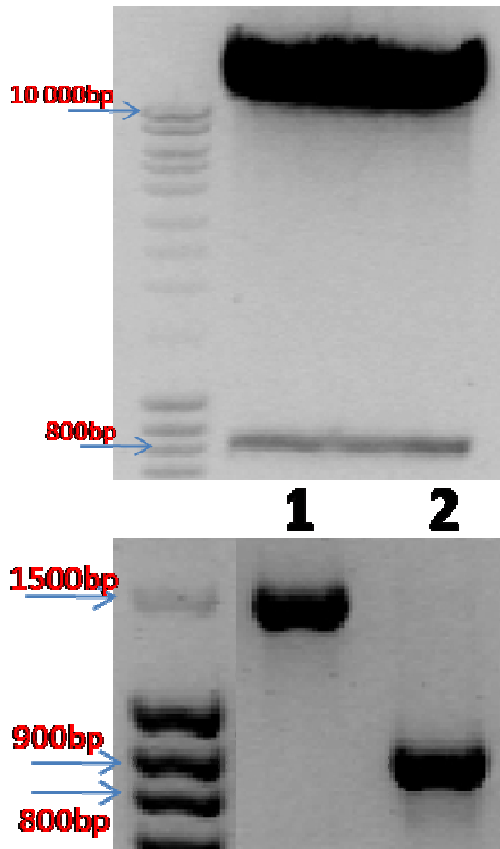


Figure 4: Illustration of pCAMBIA 1303 vector

*Pst* I and *Nco* I were used to remove the 35S promoter (Figure 5). *AtMTM1*

and *AtMTM2* promoter amplified by forward primer with *Pst* I restriction site and reverse primer with *Nco* I restriction site was inserted between those two sites. Both of the two promoters start right after the previous gene and end just before the first exon. The length of each fragment is supposed to be 1440 bp for *AtMTM1* and 880 for *AtMTM2*.



**Figure 5:** pCAMBIA 1303 was digested by *Pst* I and *Nco* I, resulting two fragments: linear vector and 35S promoter.

**Figure 6:** cloned *AtMTM1* and *AtMTM2* promoter. In lane 1, *AtMTM1* promoter(1440 bp) was shown after amplification by PCR. In lane 2, *AtMTM2* promoter was shown with 880 bp

After the promoters were amplified through PCR with Columbia 0 (Col 0) genomic DNA as template (**Figure 6**), they were treated with *Pst* I and *Nco* I in appropriate condition, and then ligated with the vector treated in the same way. Transformation was completed in *E. coli* DH5α strain. The obtained clones were verified by colony PCR (**Figure 7**). The results confirmed that cloning processes were successful and both promoters inserted into the pCAMBIA 1303 vector in which *GUS* was place under *AtMTM* promoters.

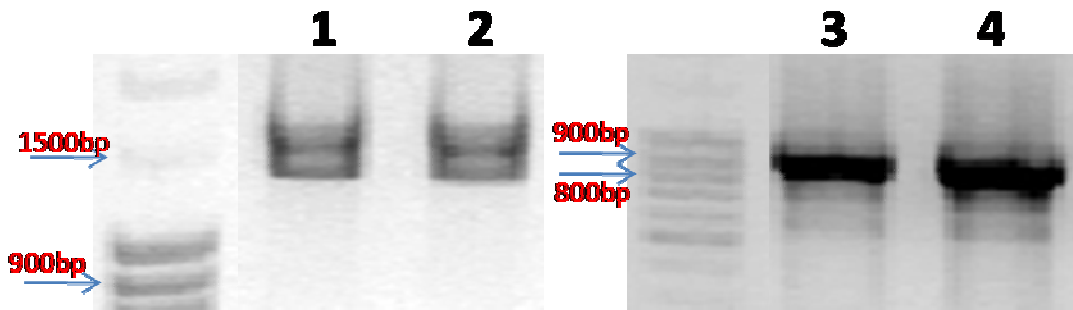


**Figure 7:** PCR results for ligation confirmation

As templates, the bacteria from transformed colonies was used in lane 2 & 4; while genomic DNA from the wt was used in first & third lanes as control. Lane 1 & 2 shared the primers of *AtMTM1* promoter, and lane 3 & 4 were amplified with *AtMTM2* promoter primers.

The plasmids containing two promoters were then transformed into Agro-bacteria by heat shock method. And then the plasmids were transformed into *Arabidopsis* (Col 0) by vacuum flower soaking method using Agro-bacteria as mediator. After 3 weeks, the seeds on the flowers soaked in Agro-bacteria were collected and sowed on hygromycin selection media. The plants survived on the antibiotic medium were further selected for the presence of GUS expression. Those lines from both *AtMTM1* and *AtMTM2* transformation showed good expression of GUS were then collected as stock. For *AtMTM1*, we finally obtained 8 lines of *AtMTM1* transgenic lines, whereas 11 lines were got from *AtMTM2*.

Seeds from line # 6 of *AtMTM1* and line # 11 of *AtMTM2* were used for the GUS expression analysis. GUS expression was present in the root, leaf, flower and silique in both *AtMTM1* and *AtMTM2* transformed plants (**Figure 8** & **Figure 9**). In **Figure 8**, the plant organs were shown developing the blue color indicating the presence of GUS. As the blue signal suggested, AtMTM1 is present in very young seedlings (**a** & **b**). Its expression level is much higher in cotyledons and relatively low in roots(**a** & **b**). AtMTM1 can be found in every leaf but much stronger expression is in the veins at early stage (**c** & **d**). Within one certain leaf, the signal was much stronger in trichomes (**e**). Also, the protein was present in flowers (**f**), especially in

pollens and stigma (**g**). Not surprisingly, this protein could be found at very old stage (**h**), too. In old plants, it was predominantly in mature siliques (**j**) and leaves which developed very late (**i**). However, there was no signal in mature stems or seeds at all (**h & i**). Since GUS expression was found through the very beginning to the final stage, and its presence was so extensive in different tissues, it was reasonable to guess that AtMTM1 might function in some development processes. This result would guide us in future study of the role of AtMTM1 in plants.

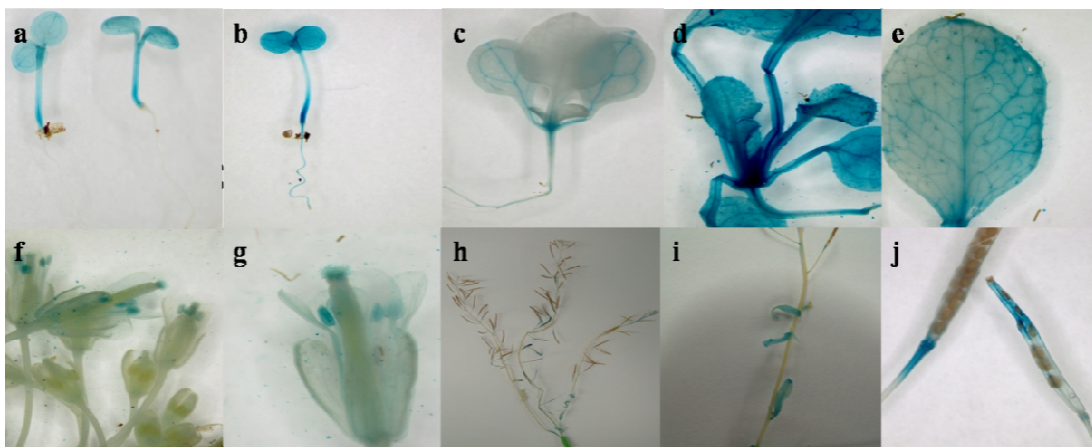


**Figure 8:** GUS expression of *AtMTM1* promoter in Col 0.  
Blue color represents the AtMTM1 expression.

Compared with AtMTM1, AtMTM2 generally had the same pattern. In our two transgenic lines, one had non-specific strong expression of GUS, which could be due to position effect; and the other showed relatively weak signal (see **i**). The stronger expression line was used to clearly illustrate the specificity of AtMTM2. AtMTM2 was almost everywhere in the plant: roots, stems, flowers and siliques; and both in young and old ages. However, there were some really interesting differences. Firstly, AtMTM2 had an obviously stronger expression in trichomes(**f**). Since it was already well known that roots shared the pattern with trichomes, this difference was again confirmed in roots (**d**). Then it could also be noticed that the color was darker in those newly developed and actively growing tissues or cells, which was illustrated in

**e, g, h, i** and **j**. These two traits might suggest AtMTM2 could play some roles in the beginning of development and differentiation processes.

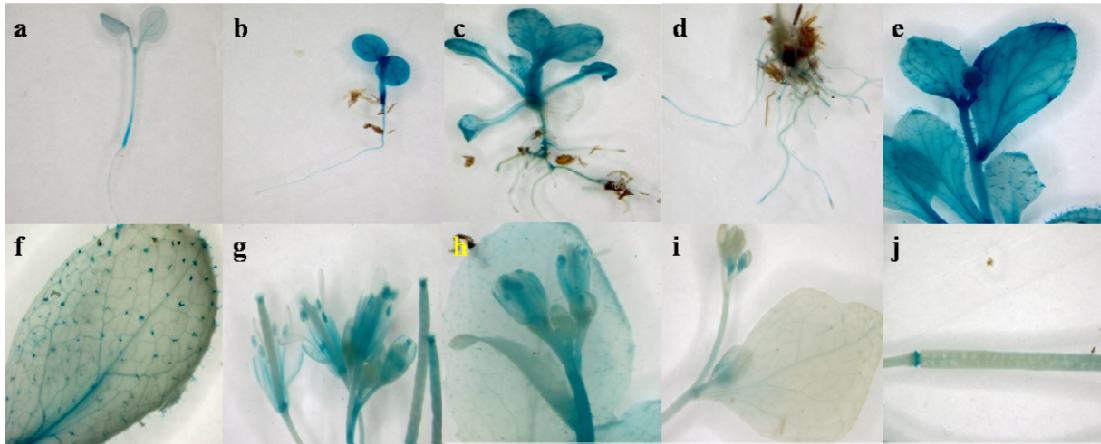


**Figure 9:** GUS expression of *AtMTM2* promoter in Col 0.  
Blue color represents the *AtMTM2* expression.

Because it is well known that the myotubularins was related to some dehydration response, it was necessary to investigate their potential expression changes under the stress. Therefore, we took the transgenic plants out of soil, left them on the table and let them dry at room temperature for 2 hours. Then the same staining procedure was applied to obtain the blue colored plants.

After treated with dehydration stress, AtMTM1 expression increased visibly in hydathodes. But no obvious change was observed in other tissues(**Figure 10**). For AtMTM2, the relatively weak expression line was stressed and observed, because the other one's signal was too strong to identify any visible increase. By contrast, AtMTM2 didn't show any responses to the stress. Its expression remained the same with that in normal condition.

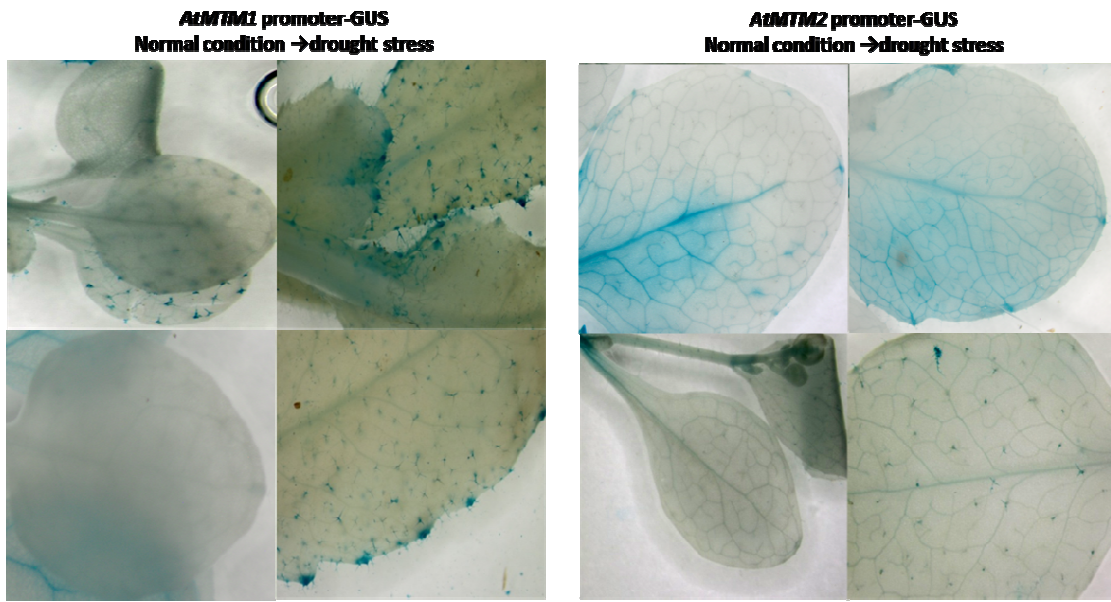


**Figure 10:** AtMTM1 and AtMTM2 expression patterns in drought condition.

### mRNA level of AtMTM1 and AtMTM2 in different tissues

The GUS blue staining method showed an overview of where AtMTM1 and AtMTM2 existed. Though comparison of the expression of each could be made across different tissues, there were several flaws of this method: first, position effect had a great influence on the GUS expression. The GUS expression level was determined not only by activity of *AtMTM1/AtMTM2*-promoter, but also by the region where the *AtMTM1/AtMTM2*-promoter GUS gene inserted in genome. Therefore, comparison between *AtMTM1* and *AtMTM2* transgenic lines couldn't reflect the difference of their promoter efficiency, because they were hardly in the same genome context due to randomly insertion. Second, even within the same line, individuals had variation. Some individuals just expressed the gene higher in certain tissues by some chances. And the last, it was not accurate at all to make a conclusion based on how strong the blue color was, which was simply observed by naked eyes.

Thus, a quantitative method was required reveal the real difference between AtMTM1 and AtMTM2 expression. That's why we employed qRT-PCR to determine

the mRNA levels of AtMTM1 and AtMTM2 next. We started with the mRNA preparation from roots, leaves, flowers and siliques of several Col 0 individuals respectively. And then the mRNA was retro-transcribed to cDNA which would be applied as common template in qRT-PCR assay. In addition, another template was made only from the leaves of drought stressed individuals. This assay was repeated for 3 times, and the mean of each was showed in **Figure 11**.

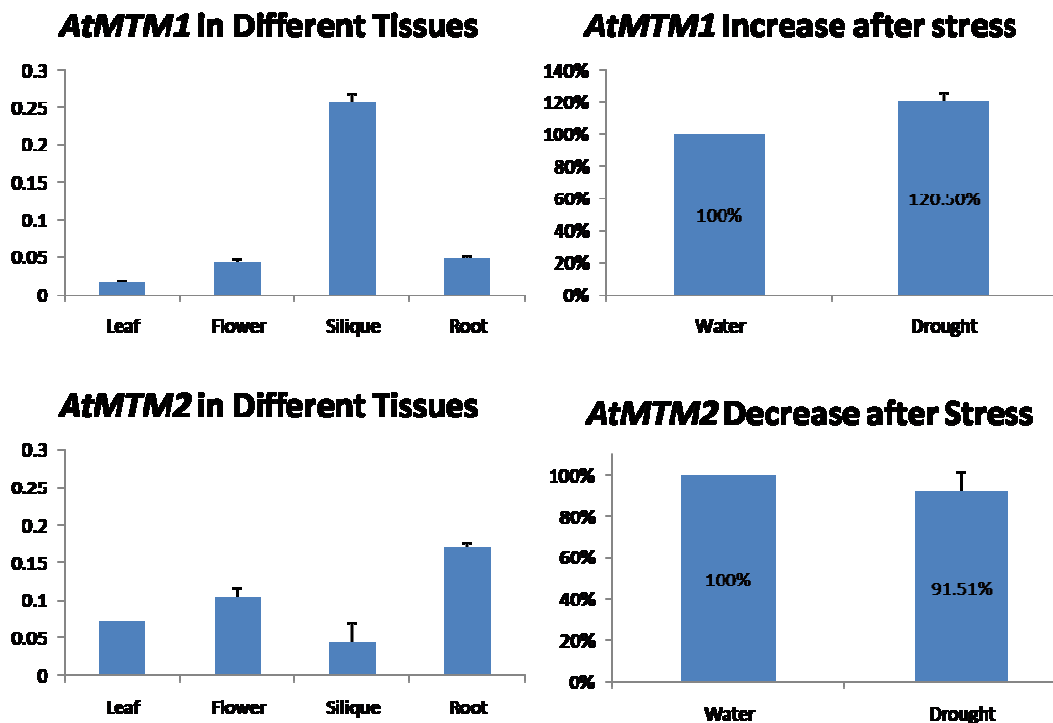


**Figure 11:** The relative mRNA amount of AtMTM1 and AtMTM2 in different tissues, and the response to drought stress

The **Figure 11** showed AtMTM1 and AtMTM2 mRNA level relative to Actin in different tissues. As can be seen, AtMTM1 was extensively expressed and much more abundant in silique than any other; whereas AtMTM2 reached its peak in root although it existed in all other tissues. Moreover, when the plants were treated with drought stress, AtMTM1 mRNA level increased by 20 percent; while AtMTM2 mRNA level decreased approximately by 10 percent if there was any real change. Although the error bar reflected there was a relatively high variation, it still proved the AtMTM2 didn't increase when the plant encountered drought stress. Again, qRT-

PCR assay confirmed the result obtained from GUS-blue staining and provided quantitative data for further analysis.

### **The subcellular localization of AtMTM1 and AtMTM2**

To study their subcellular localization, pB7RWG2.0 vector of gateway system was employed (**Figure 12**). The AtMTM1 or AtMTM2 full length CDS replaced the sequence between attR1 and attR2, respectively. Then the construct was transformed into tobacco leaves by Agro-bacteria injection. After 48 hours, we obtained the pictures showed in **Figure 13**.

In **Figure 13**, the red color represents AtMTM1 while the green color indicates the localization of AtMTM2. Transmitted pictures were also taken as negative control to illustrate the shape of the cell on the bottom. As can be seen in **a**, AtMTM1 existed mainly in cytoplasm and along cell membrane(The blue spots are chloroplasts). By contrast, AtMTM2 distributes not only on the membrane, but also in the nucleus(**b**). Another interesting difference between their localization is that AtMTM1 forms a lot small patches but AtMTM2 looks more uniform. When both AtMTM1 and AtMTM2 were transformed in a single cell(**e, f, and g**), we discovered they don't co-localize, although their colors merge into yellow along membrane. It is much clearer in picture **g** that only AtMTM2 could be found in the nucleus.

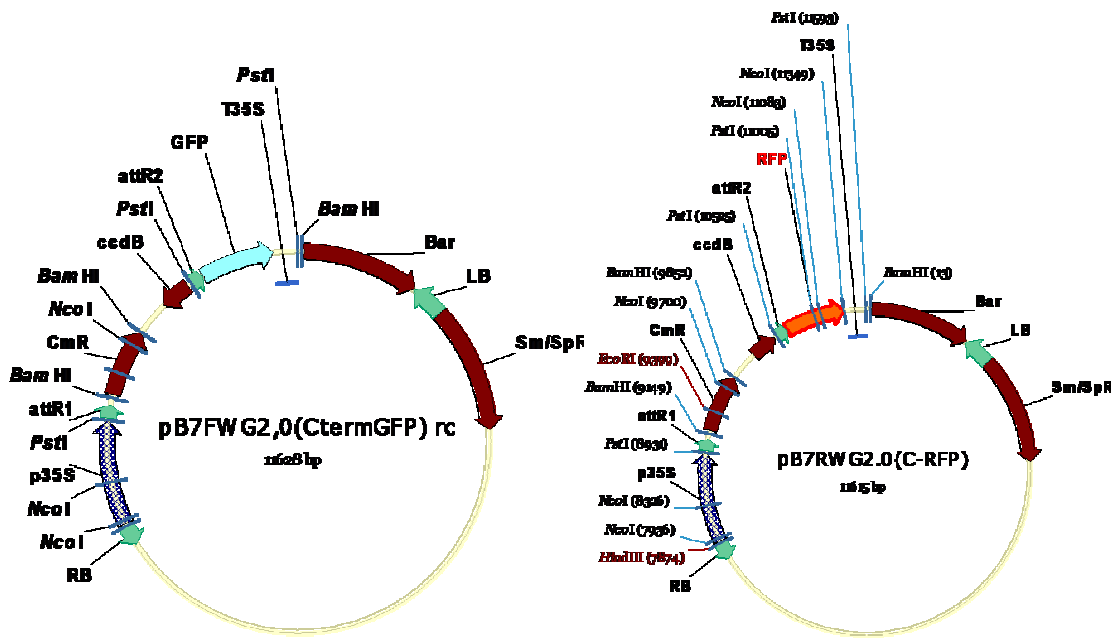


**Figure 12:** Illustration of pB7FWG2.0 C-terminal GFP/ pB7RWG2.0 C-terminal RFP vector

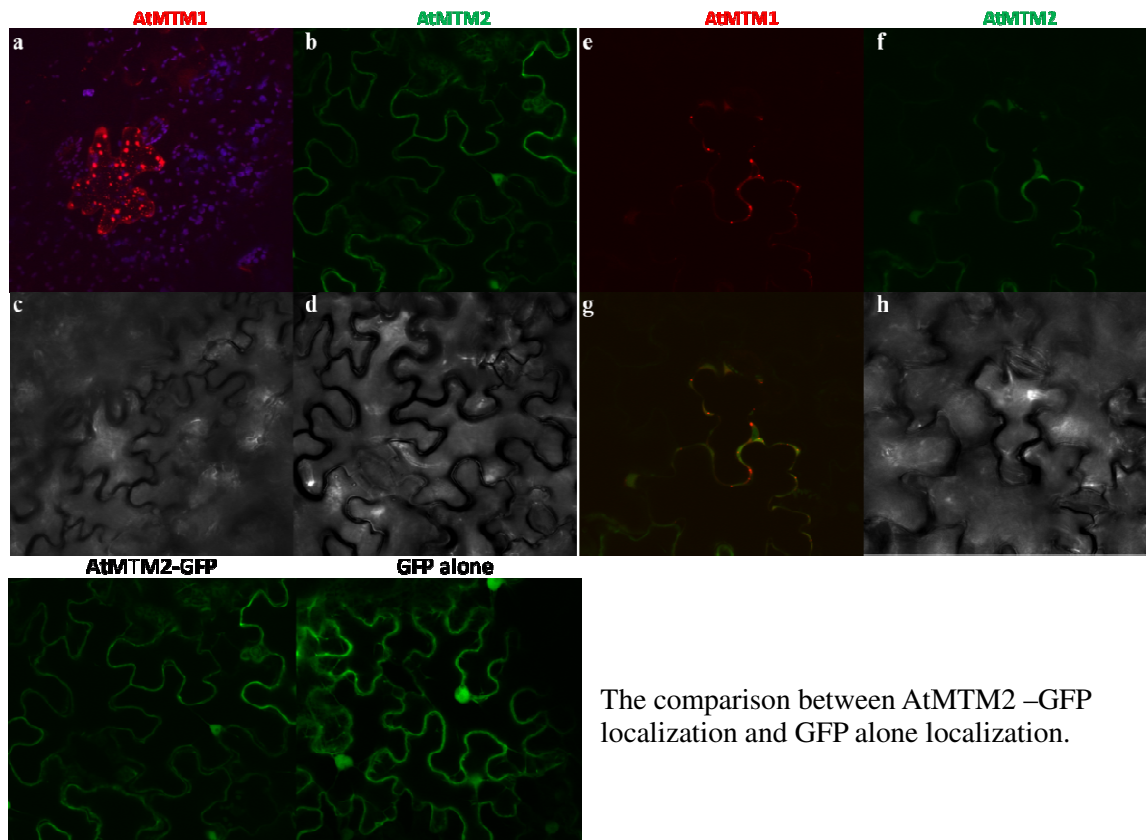


**Figure 13:** The subcellular localizations of AtMTM1 and AtMTM2. The black-white pictures are the negative control to show the cell shape.

However, since AtMTM2-GFP showed the same pattern with GFP alone.

Another possible interpretation was that AtMTM2 was lack of specificity so that it

was dragged by GFP, thus showed a same distribution pattern with GFP. Since there was a single mutation in our construct (250th amino acid: Ala(GCT) → Val(GTT)), This explanation is more plausible.

## Selection of *AtMTM1* and *AtMTM2* mutants

Several lines of T-DNA-disrupted lines of *AtMTM1* and *AtMTM2* were searched out from Salk institute genomic analysis laboratory website: <http://signal.salk.edu/cgi-bin/tdnaexpress>. There were 5 lines of *AtMTM1* mutants: SALK\_018432, SALK\_029185, SALK\_073312, SALK\_123562 and SALK\_135710; whereas 4 lines of *AtMTM2* were found: SALK\_069301, SALK\_082030, SALK\_147282 and SALK\_147338. They were bought from Salk institute genomic analysis laboratory, CA, USA. However, most of lines' seeds didn't germinate in soil or didn't contain T-DNA insertion. And the candidate *AtMTM1* mutant lines we got were: SALK\_029185 (*atmtm1-1*) and SALK\_073312(*atmtm1-2*); while only one line of *AtMTM2* mutant- SALK\_147282(*atmtm2*) was identified. The T-DNA insertion site in each of the three mutants is in the 8<sup>th</sup> exon within the PTP domain, 3'-UTR and 2<sup>nd</sup> exon, respectively. Their gene structures are illustrated as **Figure 14**.

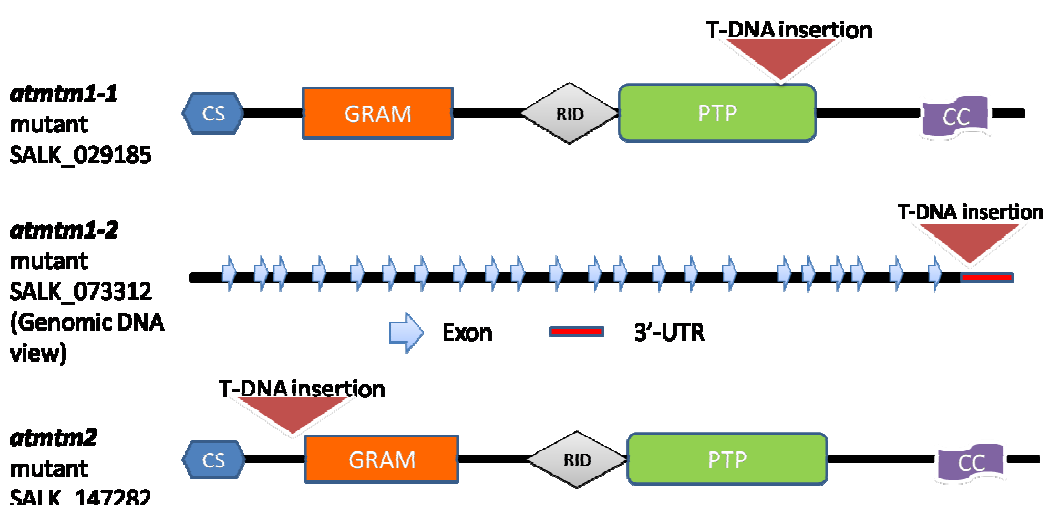


**Figure 15:** Location of insertion in *AtMTM1* in line SALK\_029185 & SALK\_073312; and in *AtMTM2* in line SALK\_147282

The insertion in the gene was confirmed using three primers for each insertion. They are Primer SALK\_029185 LP and SALK\_029185 RP, SALK\_073312 LP and SALK\_073312 RP, SALK\_147282 LP and SALK\_147282 RP, and LB-3. The LP indicates the primer complementary with sequences upstream of the insertion site; while RP means the primer complementary with sequences downstream of the insertion site; and LBb1.3 is the primer designed within the T-DNA, which is used for all the mutants screening (**Figure 12**).

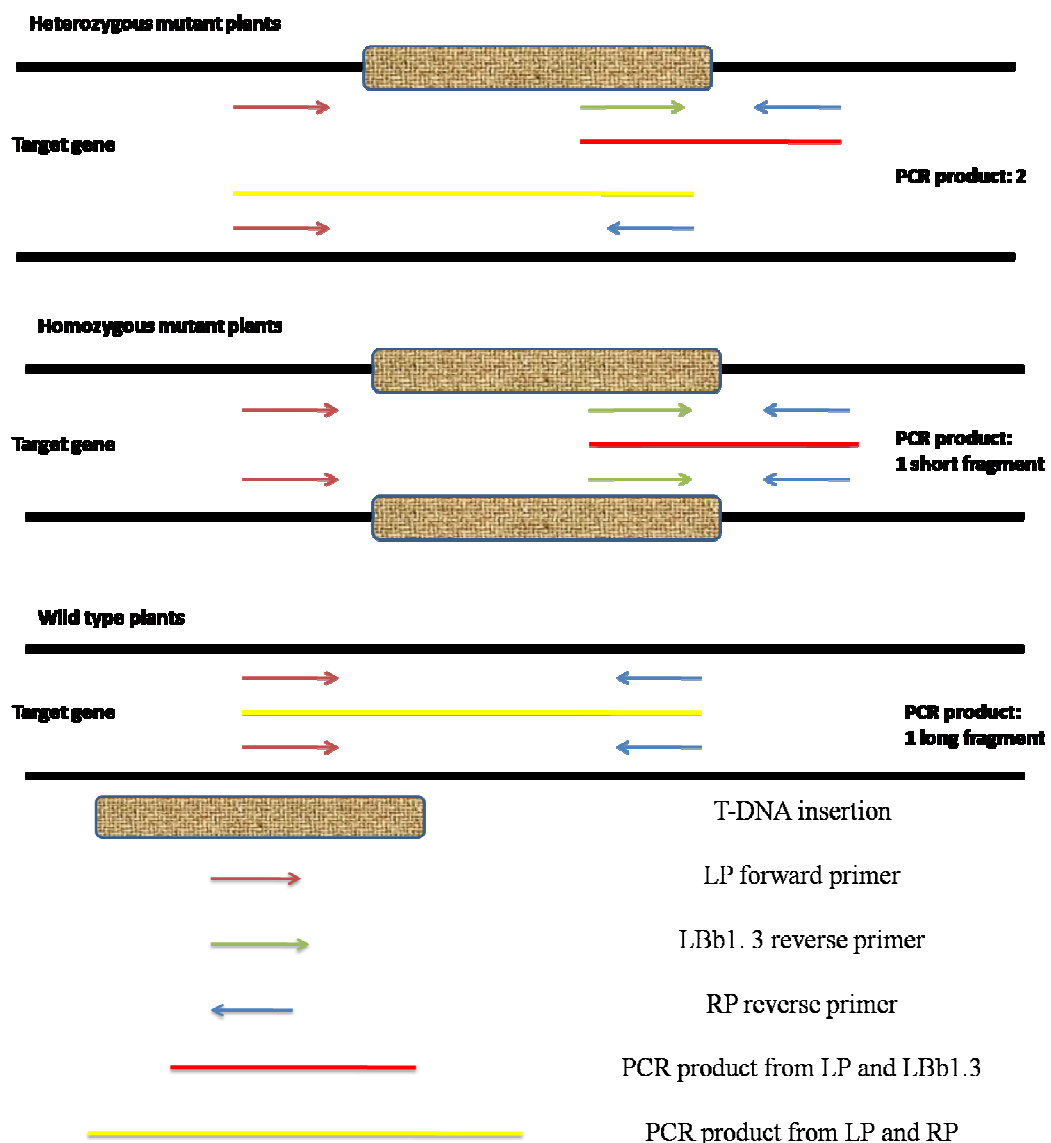


**Figure 15:** Selection of heterozygous plants versus homozygous plants by PCR. T-DNA insertion disrupts the target genes(*AtMTM1* or *AtMTM2*). The insertion is only on the one of copy of the gene, 2 different fragments will be amplified; whereas if the insertion is on both copy of the gene, only one fragment will be obtained.

The strategy for selection of the mutant lines is shown in figure 12. The purple and green arrows represent the LP and the LBb1.3 forward primers; the blue arrow is reverse primer RP. The brown region is the T-DNA insertion in the gene *AtMTM1* or *AtMTM2*. The red line shows the PCR product from a disrupted gene amplified by purple forward and blue reverse primers; while the yellow longer line indicates the fragment from a normal gene using purple forward and green reverse primers.

Both homozygous and heterozygous mutants were screened by PCR. The three primers- LP, RP, and LB-3 were added together into the reaction. Therefore, wild type (Col 0) plants should produce only one fragment after PCR, and the size for the primers of each *atmtm1-1*, *atmtm1-2* and *atmtm2* should be: 1048bp, 976bp and 1105bp, respectively. A homozygous mutant should be able to amplify only one fragment, and the size for each is 612bp, 584bp and 789 bp, respectively. However, if a mutant is heterozygous, it would contain both interrupted gene and a normal gene. Thus, this mutant would produce 2 fragments, one is around 1000bp and the other one is much shorter, and approximately between 600bp and 800bp. The result from preliminary screen for the mutants are showed in **figure 16**.

As can be seen in **figure 16**, the SALK mutant candidates were compared with wild type. *atmtm2* was prooved as a homozygous line, while only heterozygous lines were found from *atmtm1-1* and *atmtm1-2*. Unfortounately, we didn't obtain any mutants of AtMTM1 SALK\_018432 and SALK\_018431. We repeated this PCR screen again and only found 1 homozygous line of *atmtm1-2* (**Figure 17**).

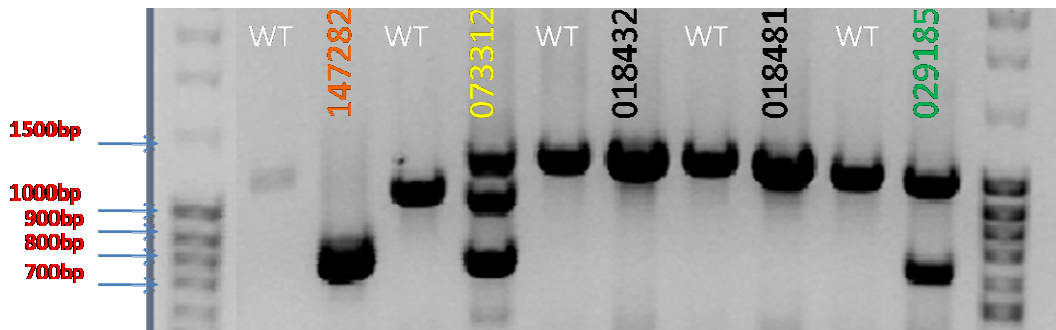


**Figure 16:** the PCR products were applied on a gel with Wild Type control beside of each line.  
**147282:** the SALK\_147282 candidate line, which turned out to be homologous mutant line of *atmtm2*  
**073312:** the SALK\_073312 candidate line, which turned out to be heterozygous mutant line of *atmtm1-2*  
**018432:** the SALK\_018432 candidate line, which turned out to be homologous wild type  
**018481:** the SALK\_018481 candidate line, which turned out to be homologous wild type  
**029185:** the SALK\_029185 candidate line, which turned out to be heterozygous mutant line of *atmtm1-1*

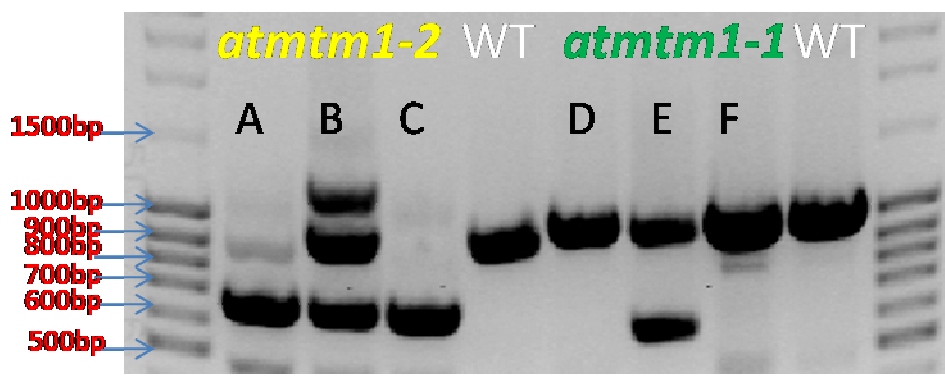


**Figure 17:** The PCR to identify homologous mutants of *atmtm1-2* & *atmtm1-1*  
***atmtm1-2*:** A & B lines were both heterozygous mutants, whereas C was the homologous mutant.  
***atmtm1-1*:** D & F lines were identified as wild type plants, whereas E was the heterozygous mutant

In order to obtain sufficient amount of homozygous mutants, offsprings of *atmtm2*, *atmtm1-1* and *atmtm1-2* were collected, and then screened again. It was expected that the offspring from a homozygous line should be all homozygous, whereas the heterozygous line would produce a mixture of homo-mutants, hetero-mutants and homo-wild types, whose ratio should be 1:2:1 according to Mendel's Law.

13 *atmtm2* and 8 *atmtm1-2* offsprings were tested to confirm they are homozygous of *AtMTM2* and *AtMTM1* mutant respectively (showed in **Figure 18 & 19**). Therefore, we got the stable homozygous *atmtm2* and *atmtm1-2* mutant lines, and we used them in the rest of studies.

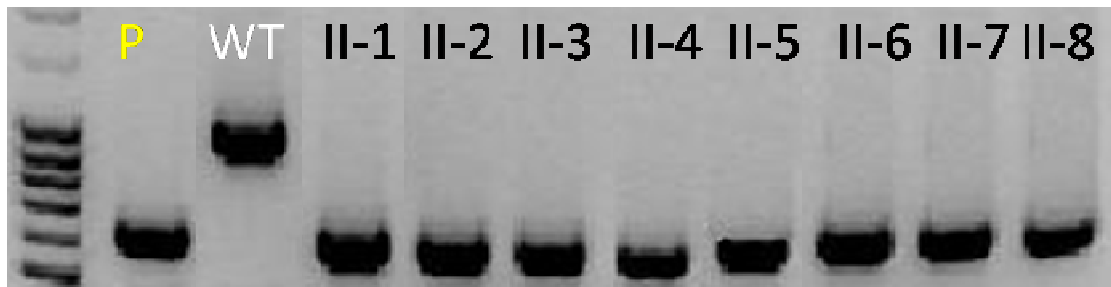


**Figure 18** : The test for *atmtm1-2* offspring.

P: The parent line, *atmtm1-2*

WT: wild type

II-1 ~ II-8: the offspring of P, all of them were homozygous mutants.



**Figure 19**: The test for *atmtm2* offspring.

P: The parent line, *atmtm2*

WT: wild type

II-1 ~ II-13: the offspring of P, all of them were homozygous mutants

And then, 24 *atmtm1-1* offsprings were tested to find out homozygous lines.

However, only 2 samples seemed like homozygous. To eliminate possible contaminations from other samples, the PCR screen was repeated with only two samples(**II-4 & II-10**). This screen showed that **II-10** was also a heterozygous mutant, and the weak band seen in **Figure 20** was not due to contamination(**Figure 21**). Only 1 offspring turned out to be homozygous mutant out of 24. This ratio was relatively lower than expectation, which indicated AtMTM1 might play some roles in seed germination or seedling survival. The offsprings produced by **II-4** self cross were also confirmed homozygous.(**Figure 22**)

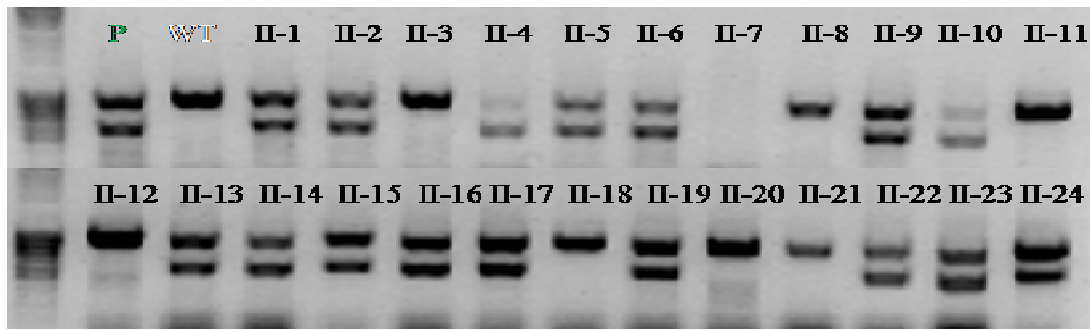


**Figure 20:** The test for HETEROZYGOUS *atmtm1-1* offspring.

P: The parent line, HETEROZYGOUS *atmtm1-1*

WT: wild type

II-1 ~ II-24: the offspring of P.

**II-4 and II-10** contained a relatively weak band around 1000bp, which could be a contamination from the lanes close to them.

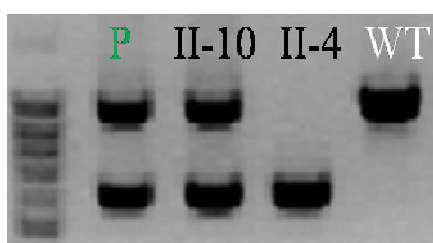


**Figure 21:** Confirmation of II-4 and II-10.

P: The parent line, heterozygous *atmtm1-1*

WT: wild type

II-10: *atmtm1-1* HETEROZYGOUS

II-4: *atmtm1-1* HOMOZYGOUS

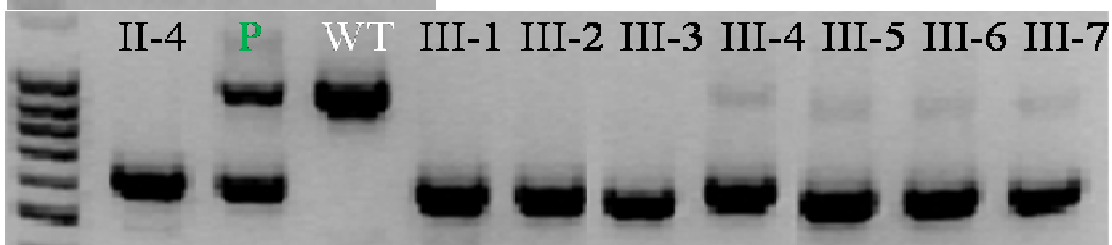


**Figure 22:** The test for II-4 offspring.

II-4: F-1 generation, HOMOZYGOUS *atmtm1-1*

P: The parent line, HETEROZYGOUS *atmtm1-1*

WT: wild type

III-1 ~ 7: F-2 generation, homozygous *atmtm1-1* mutants

Since AtMTM1 and AtMTM2 shared a lot of similarities, they might compensate each other. In this case, the effect of knock out either AtMTM1 or AtMTM2 would be weak due to their compensation; and the knock out mutant would show slight defect which could hardly be observed. Therefore it was necessary to establish a stable line of double mutant of both AtMTM1 and AtMTM2 to well know the plant myotubularin function.

We used *atmtm2* mutant as maternal plant, and pollinated *atmtm2* flower with pollens of *atmtm1-1* and *atmtm1-2* respectively. The first hybrid generation should be

all heterozygous of both *atmtm1* and *atmtm2*(Figure 23). And then Independent Assortment would occur in the next generation. According to Mendel's dihybrid rules, 1 homozygous double mutant could be found from 16 offsprings. However, the result didn't support so.

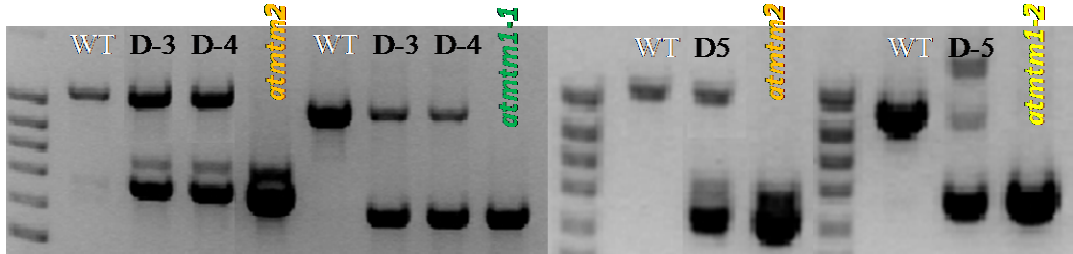


**Figure 23:** The test for double mutant *atmtm1-1* X *atmtm2* & *atmtm1-2* X *atmtm2*  
**D-3 & D-4:** the F1 generation of cross, candidates of double mutant. They were heterozygous of both *atmtm2* and *atmtm1-1*  
**D-5:** the F1 generation of cross, candidates of double mutant. They were heterozygous of both *atmtm2* and *atmtm1-2*.

Seeds of the first hybrid generation D-3, D-4 and D-5 were collected and saw. When the 2<sup>nd</sup> generation germinated and their leaves grew large enough, we screened 33 offsprings in all for homo-*atmtm2* mutants(Figure 24). Only 9 lines were found, they were line 1, 2, 27, 28-the progeny of D-5, and line 4, 5, 15, 17, 22-the progeny of D-3. Then these homo-*atmtm2* mutants were further tested for *atmtm1-1* and *atmtm1-2* (Figure 25). Unfortunately, none of them was homozygous. Line 4, 5 and 17 were both *atmtm1-1* heterozygous mutants and *atmtm2* homozygous mutants; and line 1, 2, 27 and 28 were both *atmtm1-2* heterozygous mutants and *atmtm2* homozygous mutants. And then, we had to produce the homo-double mutant from homo- *atmtm2*/hetero- *atmtm1* mutants.

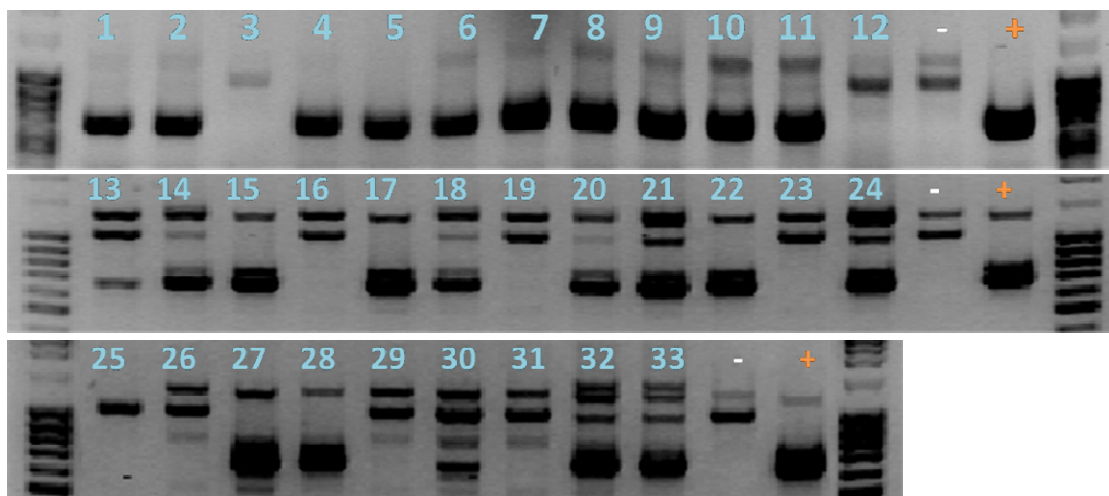


**Figure 24:** screen for *atmtm2* homozygous mutant in offspring of hetero-double mutants

-: wt negative control

+: *atmtm2* homo-mutant positive control

Only line # 1, 2, 4,5, 15, 17,22, 27, 28 were homo- *atmtm2* mutant.

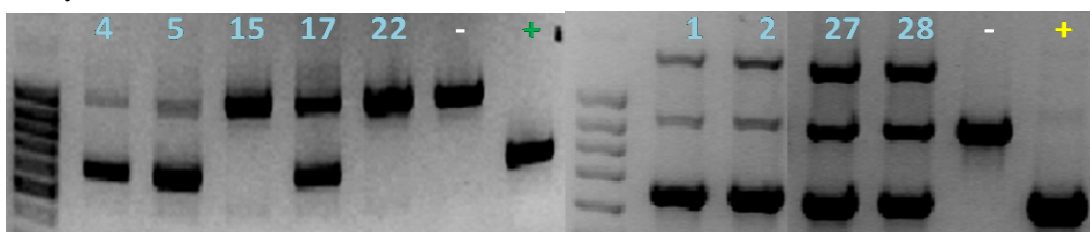


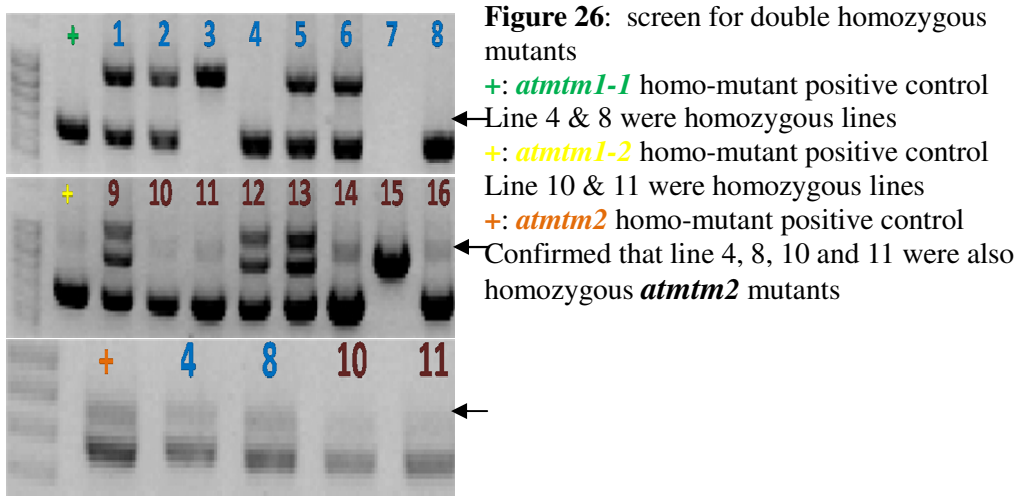
**Figure 25:** screen for *atmtm1* homozygous mutant in *atmtm2* homozygous lines(left: *atmtm1-1* & right: *atmtm1-2*)

-: wt negative control

+: *atmtm1-1* homo-mutant positive control

+: *atmtm1-2* homo-mutant positive control

Progeny from those lines were grown again to screen the homo-double mutant. At this moment, the ration of presence of a homo-double mutant is 1 to 4. As expected, we identified 2 double homozygous mutants of *atmtm1-1* and *atmtm2*, and 2 double homozygous mutants of *atmtm1-2* and *atmtm2*, from 8 offspring respectively. And their seeds were then collected as double mutant stocks.



Finally, we obtained 2 lines of homozygous *atmtm1* mutants, 1 line of homozygous *atmtm2* mutant, and 2 lines of homozygous double mutants. And also, we verified that they all had T-DNA insertions in both copies. Further studies were conducted with these mutants.

#### **Do the mutants produce any myotubularin mRNAs?**

We had proved all the mutants don't have any normal *AtMTM1* or *AtMTM2* genomic sequences. But we weren't sure whether the disrupted sequences would still be able to transcribe some message. For *AtMTM1*, the insertions in both mutant lines were relatively downstream so that there would be a high chance that *atmtm1* mutants could still produce some message RNAs. In contrast, *atmtm2* mutant had a insertion very upstream, and therefore it could hardly produce any functional messages with active site coding sequences. Thus we tested *atmtm1* mutants for both full length and truncated mRNAs, while *atmtm2* mutant was only tested for full length mRNA. Full length mRNAs were tested by pairs of primers downstream the T-DNA insertion (but upstream in *atmtm1-2*), and a pair of primers flanking the active site (upstream to the T-DNA insertion site in both *atmtm1-1* and *atmtm1-2* lines) were employed to detect truncated mRNAs. Wild type was applied as positive control. The expected RT-PCR fragments were 150 bp and 149 bp in length for *AtMTM1* and *AtMTM2* in wild type

respectively.

As result, *atmtm1* and *atmtm2* mutants showed extremely low expression of full length mRNAs(**Figure 27 A & B**). However, *atmtm1-2* did have some truncated mRNA present the test **C** even the amount was efficiently reduced compared with *atmtm2* mutant or wild type Col 0, but *atmtm1-1* contained very few. Since the primers used in test **C** were just up and down stream of the active site, this result indicated that there were probably some functional AtMTM1 in *atmtm1-2*. Then it was logical to deduce that the double mutant *atmtm1-1/ atmtm2* would lack both functional AtMTM1 and AtMTM2; whereas *atmtm1-2/ atmtm2* would have no function AtMTM2 but contain decreased AtMTM1.

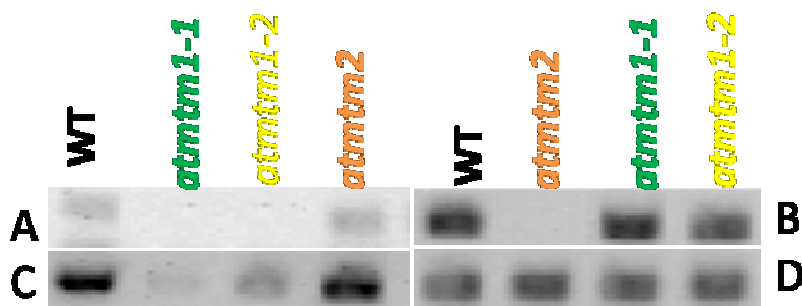


**Figure 27:** RT-PCR test for AtMTM1 and AtMTM2 messages.

- A. 150 bp. *AtMTM1* unique primers were used to detect AtMTM1 full length mRNA
- B. 149 bp. *AtMTM2* unique primers were used to detect AtMTM2 full length mRNA
- C. 340 bp. *AtMTM1* active site flanking primers were used to detect AtMTM1 truncated mRNA
- D. 150 bp. Actin loading control.

## Phenotypic Analysis

I grew 10 mutants as well as 10 wild type Col 0 as control in the same tray: *atmtm1-1*, *atmtm1-2* and *atmtm2*, respectively. After 3 weeks growth in 16 photo hour and good water condition, each of the mutants was compared with the Col 0 in the same soil. However, no significant deviations were observed at this stage (**Figure 28**).

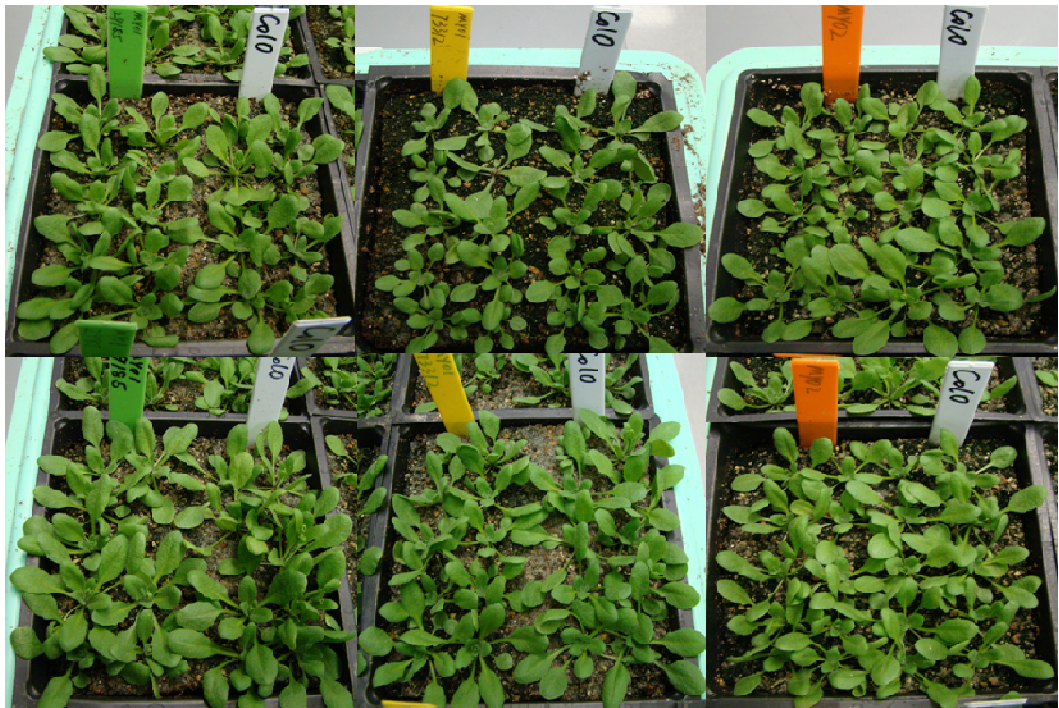


**Figure 28:** comparison between mutants and Col 0  
*atmtm1-1* VS Col 0; *atmtm1-2* VS Col 0; *atmtm2* VS Col 0

Then we stopped watering the plants and left them dry slowly in soil. The plants were observed every single day for any noticeable differences compared by the Col 0 in the same tray. Generally, no major morphological differences in leaves or flowers were found between mutant and control, except for some deviation in the flower height . And this deviation reached its peak after 5 no water days (**Figure 29**).

Those pictures showed the response to drought stress. As can be seen, *atmtm1-1* had much taller flowers than Col 0 after 5 days; while the flowers in *atmtm1-2* were a little lower if there was any difference between it and Col 0. But *atmtm2* presented almost no changes from the wild type. In day 6, 7 and 8, the plants continued dying, all leaves shrank and all stems fell down. No difference was observed during these stages. Finally, all plants got re-watered. After a week, 6 out of 10 individuals were saved from line *atmtm1-1*, while only 3 out of 10 Col 0 stood up again; *atmtm1-2* line shared the similar rescue number with its control: 6 and 7 out 10; and number of saved *atmtm2* mutants was smaller than that of wild type by only 1, too, which was 4

compared with 5.

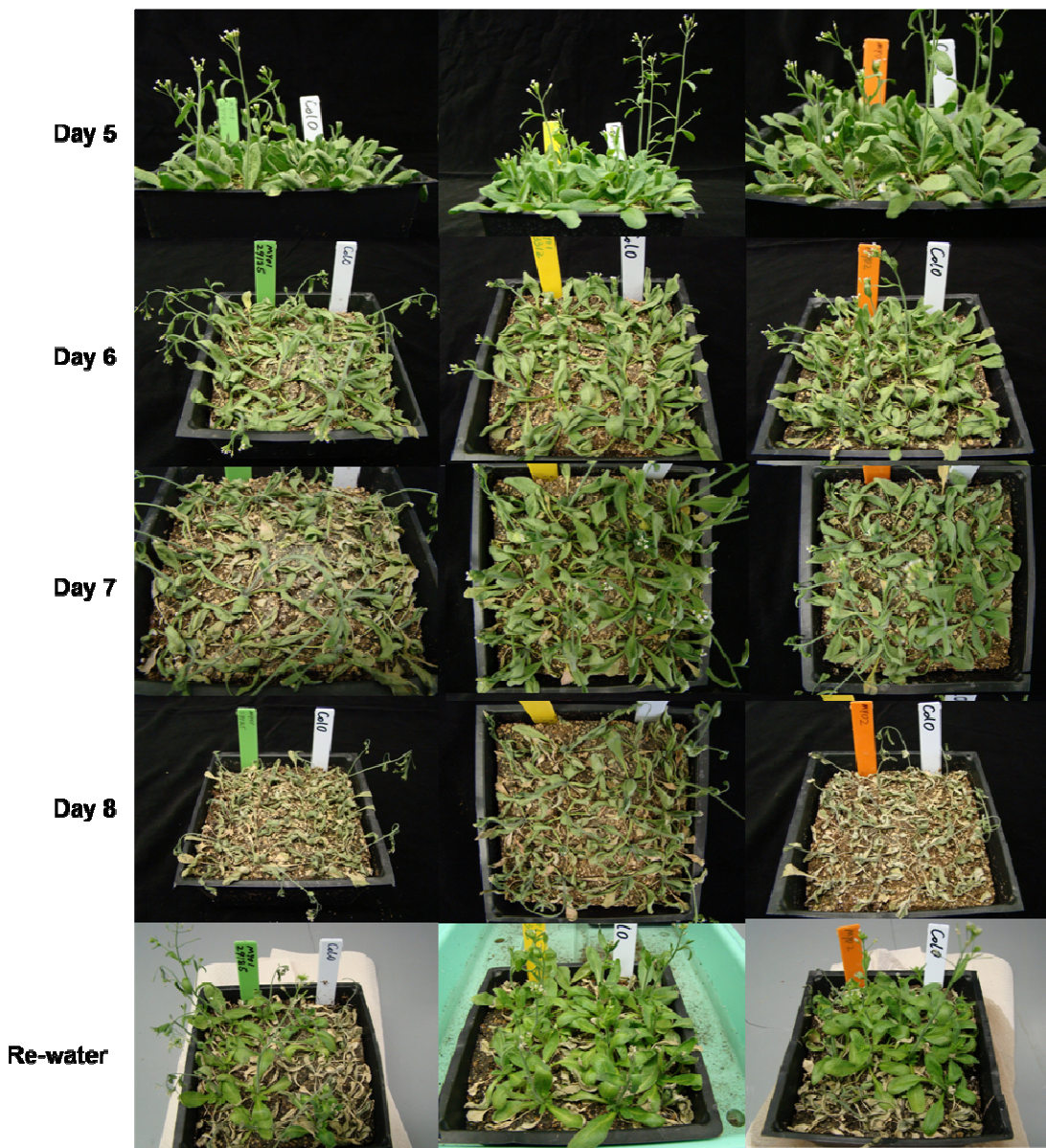
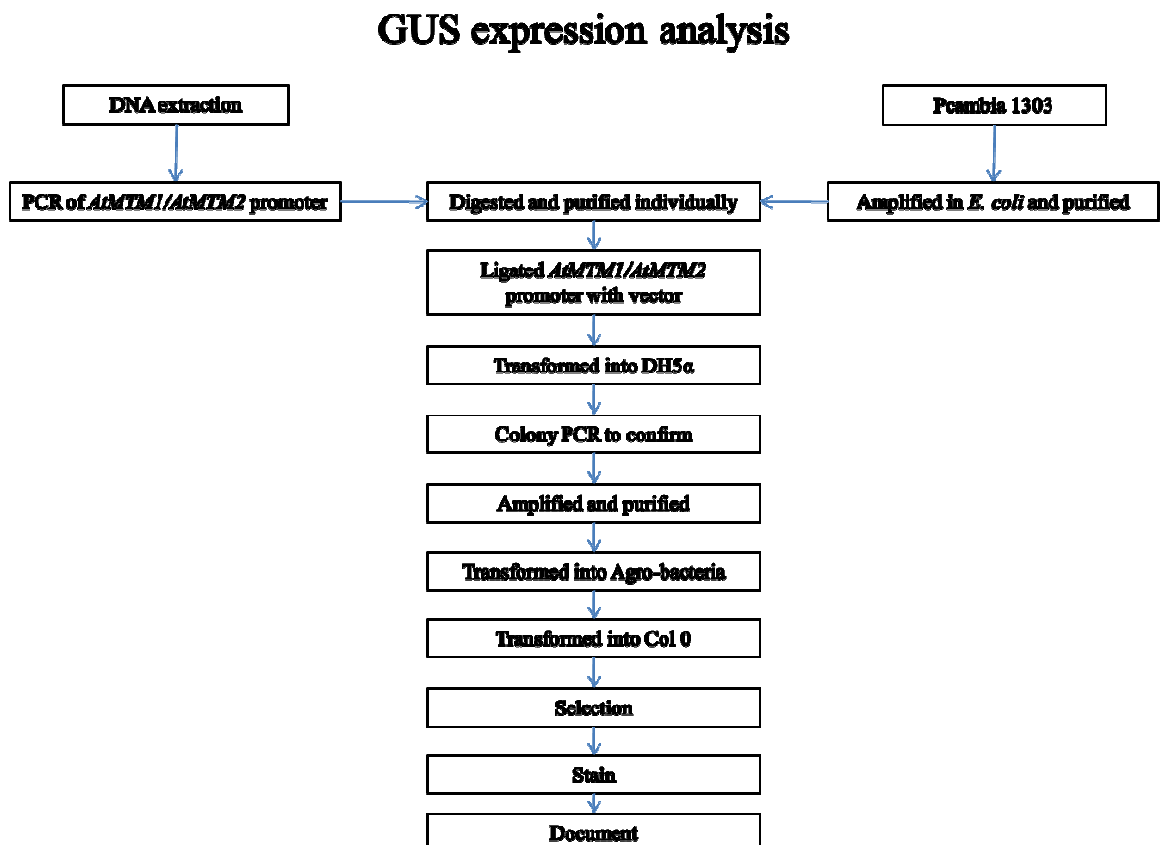


**Figure 29:** The phenotypic response to drought stress of *atmtm1* and *atmtm2* knockout mutants.

## MATERIALS AND METHODS

### 1. GUS Expression Analysis

The procedure of GUS Expression Analysis is illustrated in **Flowchart 1**, below:



**Flowchart 1:** Schematic illustration of the experimental procedures for GUS expression analysis

#### 1. 1. Amplification of promoter sequences

Genomic DNA was extracted from leaves of Col 0 plants. The leaves were ground in liquid nitrogen, and then dissolved in CTAB (Cetyl trimethylammonium bromide) solution. Same volume Chloroform and double volume ethanol were then applied to purify and precipitate the DNA. After washing with 75% ethanol (twice), the DNA was finally re-suspended in 50ul double-distilled water.

The respective primers for the *AtMTM1* and *AtMTM2* promoters were designed for the same annealing temperature, as suggested (Integrated DNA Technologies, IA, USA). The *AtMTM1* forward primer contained a *Pst* I restriction

site and the reverse primer had an *NcoI* restriction site. Primer sequences are shown in Table 1 below. Four extra nucleotides were added at the 5 prime ends of both primers to serve as protective bases. The forward primer for *AtMTM2* had a *HindIII* restriction site, while the reserve primer had an *NcoI* restriction site. Two protective bases were added to each of the *AtMTM2* primers.

ATMTM1AAFprompstF	aatt <u>CTGCAGGAATTGAAGAAG AAGAAA AGAGGA AGCT</u>
ATMTM1GRAM promncoiR	aatt <u>CCATGGAAAAAGGGGGAGAGAAAGAGAC</u>
ATMTM2-PROMOTER-F	at <u>AAGCTTAGCTGCCAAGAGAAGA</u>
ATMTM2-PROMOTER-R	at <u>CCATGGTAAAAAGGAGAGAGA</u>

**Table 1:** primer sequences for promoter amplification  
 PCR reactions were carried out for 35 cycles at 94°C for 30sec, 55 °C for 30 sec, and 72 °C for 1 min, with Taq polymerase (Fermentas cat# EP0402) on the machine RoboCycler Gradient Temperature Cyclers (Strategene). The composition of reaction mixture was exactly the same as described in the manual. Amplified fragments were run on 1% agarose gel stained by ethidium bromide (final concentration 0.5 ug/ml). The fragments were removed from the gel under UV light and extracted from the gel by using Promega wizard SV Gel and PCR Clean Up System (cat#A9281). Fermentas FastDigest® *PstI*(cat#FD0614) and FastDigest® *NcoI*(cat#FD0574) restriction enzymes were used at 37°C for 30 min to completely digest *ATMTM1* promoter in fastdigest green buffer; FastDigest® *HindIII* and FastDigest® *NcoI* were used under the same condition for *AtMTM2*.

## 1.2. Preparation of pCAMBIA 1303 for ligation

pCAMBIA 1303 plasmid (CAMBIA, Canberra, Australia) was used to transform, by heat shock, E.coli DH5α chemically competent cells: after mixing with 5μl DNA, the cells were left on ice for 40 min, followed by exposure to 42°C (in water bath) for 90 sec, placed on ice for 5 min and allowed to recover from the shock

in LB medium without antibiotics, for 40min at 37°C. After these treatments, cells were spread on plates with LB medium containing Kanamycin. The transforming vector was amplified in LB broth, at 37°C with shaking, purified by the Promega kit Wizard® Plus Minipreps DNA Purification System (cat#A7510), and treated with the two pairs of restriction enzymes as described above.

### **1.3. Ligation, confirmation of ligation, amplification of the constructs, and transformation into Agro-bacterial**

After purification, the double digested promoters were ligated to the vectors. Ligation was carried out overnight, at 16°C, by the Fermentas T4 DNA Ligase (cat#EL0011). The ligated constructs were next transformed into DH5 $\alpha$  competent cells by the heat shock method, and selected on Kanamycin plates as described above.

To confirm that the transformed cells contained the required sequence, the colonies grown on the plates overnight were suspended in 30ul water and a 5ul sample of this suspension was used as a template to be amplified by PCR with the respective primers for *AtMTM1* or *AtMTM2*. Presence of a DNA fragment in the amplified sample corresponding to the original DNA fragment used to transform the cells would identify a positive colony. Positive clones were grown in 10ml LB overnight, and used to extract the amplified amount of recombinant constructs.

The recombinant constructs were transformed then into Agro bacteria (C58C1 strain) by the heat shock method, as follows: the cells and DNA were place on ice for 5min, immersed in liquid N2 for 5min, incubated in water bath at 37°C for 5min, and then grown in DYT medium, without any antibiotics, for 2 hour at room temperature. Lastly, the cells were spread on plates with Rifampicin, Gentamycin and Kanamycin (Wise, Liu et al. 2006). It took 3 days for the colonies to grow large enough to be observed.

#### **1.4. Plant transformation and selection**

*Arabidopsis thaliana* ecotype Columbia 0 (Col 0) was used as a background transformation system. The promoter-GUS constructs were transformed by dipping of developing floral tissues into a solution containing transformed *Agrobacterium tumefaciens*, 5% sucrose and 500 microliters per litre of surfactant Silwet L-77 (Clough and Bent 1998).

Treated plants were placed back in the green house until they developed seeds. The seeds from the dipped flowers were collected and sewn on MS medium containing Hygromycin. Surviving plants were transplanted onto regular (metro mix) soil in pots. Selected tissues, or whole plants, were stained in the X-Glu solution at 37°C overnight. After washing with 75% ethanol, successfully transformed plants show blue color. Positive lines were kept as stock, and their offsprings were used in subsequent studies

#### **2. Dehydration Stress Treatment**

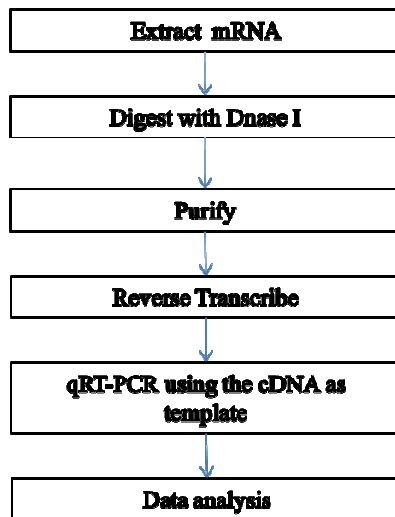
Air drying was used in GUS expression assay and qRT-PCR test. The plants were intact taken out from the soil, and then left on the table at room temperature for 2 hours. Other procedures specific to each assay were then applied to the treated plants.

Soil-drought treatment was introduced to determine the phenotype of mutants. After 18 days growing, the rectangular bows in which the mutants were along with wild type were taken out from water tray. Three days later, the soil in the bows became dry and drought stress started then. Phenotypic changed was then observed and documented every day.

#### **3.Determination of mRNA Levels by qRT-PCR**

The procedure is illustrated in **Flowchart 2**, below:

## Quantitative Test of mRNA level



**Flowchart 2:** Schematic illustration of the experimental procedures for qRT-PCR analysis

### 3.1. mRNA preparation

Total RNA from the roots, leaves, flowers and siliques of non-stressed (watered) Col 0 or mutant plants, as well as dehydration stressed experimental samples were extracted using the Trizol Reagent (Invitrogen cat#10296-010). DNase I (Fermentas cat# EN0521) was used to eliminate possible DNA contamination from the total RNA samples. Reverse transcription was done with SuperScript® III Reverse Transcriptase (Invitrogen cat#18080-044). Total of 5ug RNA was used in each reaction. The cDNA obtained from the reverse-transcription was diluted to 100ul final volume in water. qRT-PCR was performed with 5ul cDNA as a template for each sample.

### 3.2. The qRT-PCR assay

qRT-PCR was carried out in the SYBR Green kit (Invitrogen cat#11735-032). The parameters for the reaction were: 95°C for 30sec, 55°C for 30sec and 72°C for 30sec, until the signal could be detected. The *AtMTM1* and *AtMTM2* primers are shown in Table 2 below:

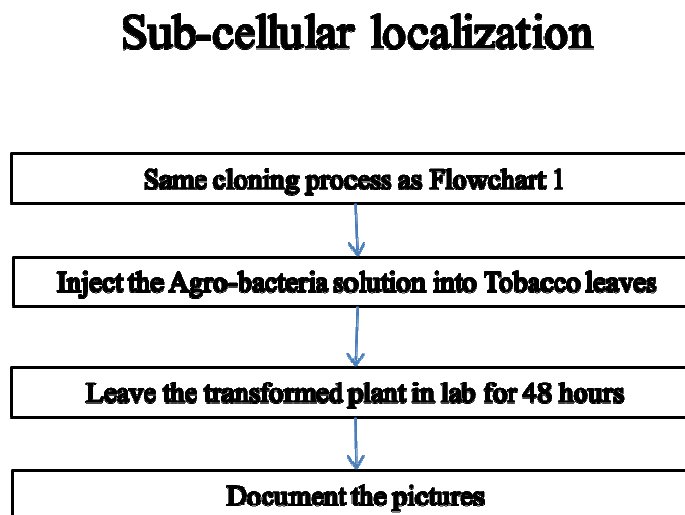
ATMTM1 RT vs2 F	GATTAACCAACCACATCTGATGTCG
ATMTM1 RT vs2 R	CCCTTCGGGTTCCAGATG
ATMTM2 RT vs1 F	CACAAGAACGGAGATTGCACAG
ATMTM2 RT vs1 R	CACACTGCTCACACACATTGTTC

**Table 2:** primer sequences for qRT-PCR test to compare *AtMTM1* with *AtMTM2*

The reactions for AtMTM1 and for AtMTM2 were done in triplicates. The mean from the 3 measurements was used in the data analysis. Relative amount of AtMTM1 or AtMTM2 in each tissue was calculated as  $2^{(C_{actin} - C_{AtMTM1})}$ . In this equation, the Cactin represented the cycle numbers of actin control, while Cmyo meant the cycle numbers of *AtMTM1* or *AtMTM2* in each tissue. This test had been repeated three times with the same mRNA samples.

#### 4. Transient Expression of AtMTM1 and AtMTM2 in Tobacco Leaves

The procedure is illustrated in **Flowchart 3**, below:



**Flowchart 3:** Schematic illustration of the experimental procedures for cellular distribution

To reveal the intracellular localization of the AtMTM1 and AtMTM2 proteins, we generated constructs expressing either one as a fusion protein with the Green-, or Red-, Fluorescent Protein, GFP, or RFP, respectively. The intracellular distribution of fluorescently tagged AtMTM1 or AtMTM2 was observed under confocal microscope.

For each sample, pictures were shot in green channel, red channel, blue channel for the chloroplast as control, and in the 3 together. Also, transmitted images were taken without fluorescence to show the cell shape.

#### 4.1. The Gateway cloning process

Full length cDNA sequence(CDS) of AtMTM1 and AtMTM2 were amplified by PCR with cDNA from Col 0 as template. Reaction was performed as 35 cycles at 94°C for 30sec, 50°C for 30 sec, and 72°C for 1.5 min, with pfu (Fermentas cat# EP0501). The primers used for each were shown in Table X below:

ATMTM1 attB1CDS	<i>attB1</i> -ATGGATATGATTGAAGATGGTGCG
ATMTM1 attB2CDS	<i>attB2</i> -TTTAGGTTGAAATAGCTATCGTAGATG
ATMTM2 attB1CDS	<i>attB1</i> -ATGACGGCGCTGAGACCTCT
ATMTM2 attB2CDS	<i>attB2</i> -TTCAGCTGTGAAATAGCTGTCGTAGAC

(*attB1*: GGGGACAAGTTGTACAAAAAAGCAGGCT;

*attB2*: GGGGACCACTTGTACAAGAAAGCTGGGT)

**Table 3:** primer sequences for CDS with attachment B site

After purification, the PCR fragments were recombined with pDONOR 221 vector (which can only be amplified in *E. coli* D.B. 31 strain) to form the ‘entry clone’ by the recombination reaction between attachment sequence “B” site in the fragments and attachment sequence “P” site in the pDONOR 221 vector, which is so-called “BP” reaction. This reaction was carried out under the recommendations of Gateway® BP Clonase® enzyme mix(Invitrogen cat#11789-013). The entry plasmids were amplified in DH5α. Next, the entry plasmids were mixed with the destination vector pB7RWG2.0 C-terminal RFP- or GFP- vector to perform another recombination reaction between attachment sequence “L” site in the entry plasmid and attachment sequence “R” site in the destination vector, which is so-called “LR” reaction. After the LR reaction, CDS sequences with attachment borders were inserted into destination

vectors. Gateway® LR Clonase® enzyme mix(Invitrogen cat#11791-019) was used to perform this reaction. Then the constructs were transformed into DH5 $\alpha$  competent cells.

#### **4. 2. Transformation of the constructs into Agro bacteria**

The same procedure was followed as described above in (1.3.).

#### **4.3. Transformation of tobacco leaves**

Agrobacteria was grown overnight at 30oC in 10ml DYT with antibiotics (Rifampicin, Gentamycin and Spectromycin). The cells were collected and re-suspended in an equal volume of induction medium (60 mM K<sub>2</sub>HPO<sub>4</sub>, 33 mM KH<sub>2</sub>PO<sub>4</sub>, (NH<sub>4</sub>)SO<sub>4</sub>, 1.7 mM Na Citrate.2H<sub>2</sub>O, 10 mM MES, 1 mM MgSO<sub>4</sub>, 0.2% Glucose, 0.5% Glycerol, antibiotics and 50 mg/ml of acetosyringone), and induced with shaking for 6 hours at 30°C. After 6 hours, the cells were diluted to an OD of 0.5 in infiltration medium (0.56 MS, 10 mM N-moropholino-ethanesulfonic acid, 150 M acetosyringone) and used to inject the abaxial surface of *N. benthamiana* leaves.

After approximately 40 hours, detection of expression was conducted by laser scanning confocal microscopy using 488- and 633-nm excitation and two-channel measurement of emission, 522 nm (green/GFP) and 680 nm (red/chlorophyll). RFP was detected by excitation at 540 nm and emission at 590 nm (Ndamukong, Jones et al. 2010).

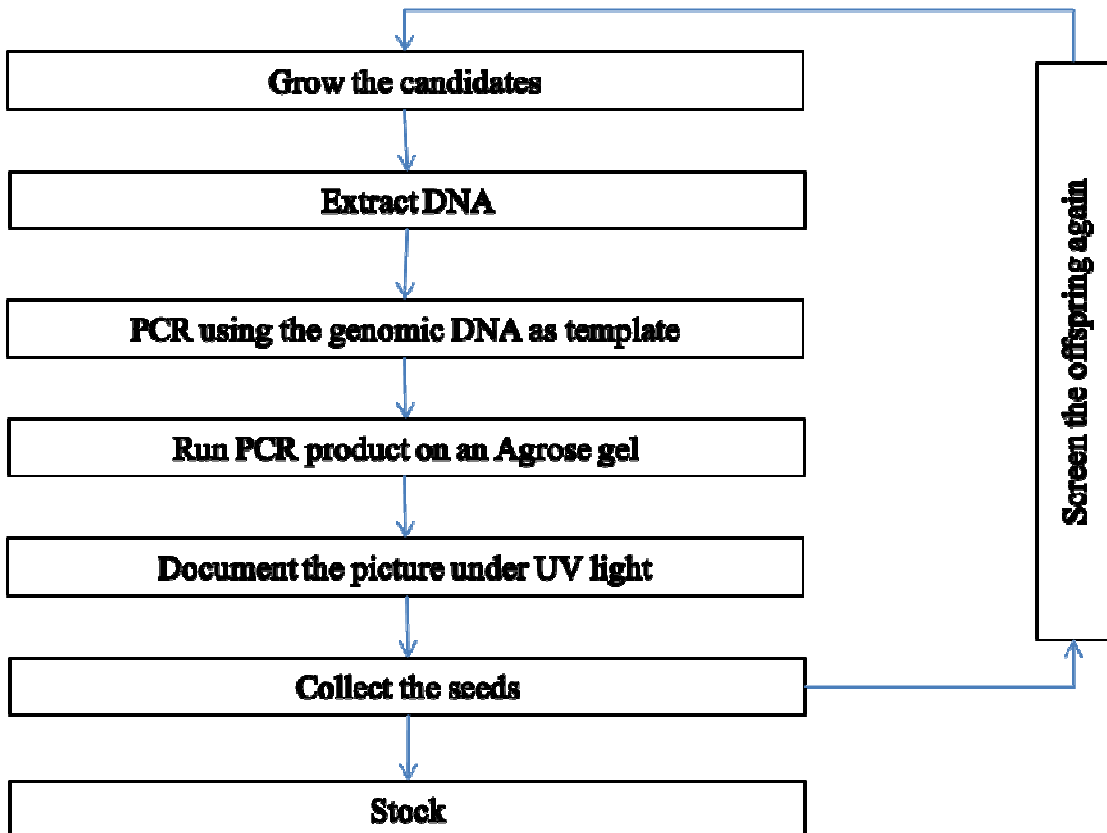
### **5. Selection for Mutants and Phenotype Screens**

#### **5.1. Selection of atmtm1 and atmtm2 mutant lines**

T-DNA disrupted myotubularin lines were obtained from the SALK Institute (Salk Institute Genomic Analysis Laboratory, CA, USA). Approximately 10 seeds of each line were received from the institute. The seeds were sown on to the Metro Mix soil. However, some seeds didn't germinate. Those survived individuals were further

tested by PCR for their genotype of *AtMTM1* or *AtMTM2*.

## Selection of mutants



**Flowchart 4:** Schematic illustration of the experimental procedures for mutants identification

Genomic DNA samples were extracted and purified as described above in **1. 1.**

Amplification was performed using 35 cycles of 95°C for 30sec, 55°C for 30sec, and 72°C for 1min with Taq polymerase (Fermentas cat# EP0402). Amplified fragments were run on 1% agarose gel stained by ethidium bromide. Pictures were taken under UV light by Bio Rad Gel Doc 2000 System PC/MAC RS-170. The LP and RP primers of each mutant are shown in **Table 4** below and the primer in T-DNA was: LBb1-3(ATTTTGCCGATTCGGAAC):

Salk_147282 LP	TTTTATGAAAAAGAGACAAATTCC
Salk_147282 RP	CAAGTGGAAACAAGCTTCTGG

Salk_073312 LP	TCACTCGGGTGCAAGATTAAC
Salk_073312 RP	CGTAGGTTCTTCTCCGATCC
Salk_018432 LP	TCTGCCAACCCATTGAAATAG
Salk_018432 RP	GATGGGAGATCATCGTTCTTG
Salk_018481 LP	TCTGCCAACCCATTGAAATAG
Salk_018481 RP	GATGGGAGATCATCGTTCTTG
Salk_029185 LP	GCTGTGAAACGCTATCAATCC
Salk_029185 RP	TGTGAATTCTGCAGAGACACCG

**Table 4:** LP and RP primer sequences for mutants screen

Lines carrying the T-DNA insertion were isolated and selfed and their offspring (F2) were tested for homozygosity. To confirm, samples of the F3 generation were re-tested. Seeds from established homozygous lines were stocked for further experiments.

### 5.2. Confirmation for disrupted *AtMTM1* or *AtMTM2* sequences

Total RNA from the leaves of Col 0, *atmtm1-1*, *atmtm1-2* and *atmtm2* were extracted, digested and reverse-transcribed as described before (see chapter 3.1.). Five ul cDNA aliquot of each sample was used as a template in the RT-PCR assay. The reactions were carried out at 95°C for 30sec, 55°C for 30sec, and 72°C for 30sec for 30 cycles with Taq polymerase (Fermentas cat# EP0402), along with Actin as control. Finally the result was documented by Bio Rad Gel Doc 2000 System PC/MAC RS-170. The primers used were specific for *AtMTM1* or *AtMTM2* despite the high level of similarities of their CDSs.

<i>ATMTM1</i> RT vs2 F	GATTAACCTCACCATCTGATGTCG
<i>ATMTM1</i> RT vs2 R	CCCTTTCGGGTTCCAGATG
<i>ATMTM2</i> RT vs1 F	CACAAGAACGGAGATTGCACAG

ATMTM2 RT vs1 R	CACACTGCTTCACACACATTGTTC
ATMTM1 ACTIV F	CAATGAGGGAGAGCTTTCCCG
ATMTM1 ACTIV R	AGCCTGAAACCCAGCAAAAGTTC

**Table 5:** primer sequences for RT-PCR of *AtMTM* messengers

### 5.3. Screening for mutant phenotypes

Homozygous mutant plants confirmed by PCR were grown in Metro Mix soil along with Col 0 in small trays. In each small tray, there were in all 10 mutants as well as 10 wild type plants growing in parallel. Growth conditions were 16 hour day/8 hours dark, at 28°C, in the greenhouse. When plants were 3 weeks old, drought stress was introduced. Mutant plants phenotype in both normal and drought conditions were documented compared to the wild type Col 0.

## 6. Generating Double Mutants for *atmtm1/atmtm2*

Homozygous single *atmtm1* and *atmtm2* mutants were grown on Metro Mix soil for 3 three weeks. Before the buds bloomed, the stamens of *atmtm2* flowers were removed from the buds. Pollen collected from *atmtm1-1* or *atmtm1-2* mutants was used to pollinate the stigmas in *atmtm2* buds. If pollination was successful, siliques would develop in three days. Upon their maturation, we collected the seeds from cross-pollinated siliques and F1 samples were tested to confirm heterozygosity for both *atmtm1* and *atmtm2*. Subsequently, F2 was screened for homozygous **double mutants** using the same strategy as described above in chapter **5.1..**

## DISCUSSION

Myotubularin is widely accepted for the function in signal transduction. We focused on AtMTM1 and AtMTM2 because they are homologs of human MTMR2, but scarcely studied in plants. Previous research showed AtMTM1 is capable of produce PI5P both in vitro and in vivo, and also responsible for PI5P increase under stress (Ndamukong, Jones et al. 2010). By comparing AtMTM2 with AtMTM1, we shall expand the knowledge on the function of related, but distinct, members of a plant myotubularin family.

### **Tissue specific expression of *AtMTM1* and *AtMTM2* in *Arabidopsis***

To reveal the tissue specific expression of the *AtMTM1* and *AtMTM2* genes, we illustrated GUS expression in transformed plants. We studied the tissue specificity of both gene expressions by following the expression of GUS under the full promoters of each gene in transgenic *Arabidopsis* lines. The *AtMTM* promoters were cloned upstream of the GUS reporter gene and GUS expression was observed in various plant tissues. For both *AtMTM1* and *AtMTM2* genes, expression was seen in leaves, in roots, in flowers and in siliques. This result is in agreement with the discovery that PI5P is ubiquitously present in the plant (Ndamukong, Jones et al. 2010).

An important character of AtMTM1 expression should be noted is, AtMTM1 is more abundant in newly synthesized tissues and actively developing cells. It was reported that the level of PI5P is not constant during cell cycles. Therefore our result confirms this observation that there is a obvious difference in the PI5P level between the cells in different development state. And the cellular PI5P change is close related to the myotubularin-AtMTM1, again suggesting PI5P plays a significant role in PI5P metabolism.

In comparison, AtMTM2 is also expressed in all tissues. But more specifically,

it presents a much stronger expression in roots and trichomes. This difference from AtMTM1 indicates a potential function of AtMTM2 in water absorption trafficking in the roots.

Their expression after being exposed in air for 2 hours is crucial to our studies. Surprisingly, AtMTM1 showed a visible increase, particularly in the hydathods while there was no change on AtMTM2 expression. This result confirmed the function of AtMTM1 in PI5P increase under osmosis stress. Also it aroused an interesting question that what does AtMTM1 or PI5P do in hydathods. A hydathod is a special secretory gland locates in the epidermis or margin of leaves. Its main function is to secret water through the pores. The appearance of AtMTM1 in this organ relates AtMTM1 directly to the drought response in plant. So a model that AtMTM2 primarily control water absorption in roots, while AtMTM1 regulates water secretion in leaves, occurs to our mind. Further studies should address their potential functions in the both pathways and verify this hypothesis based on their tissue specificity.

### **Quantitative test of *AtMTM1* and *AtMTM2* after dehydration**

To determine *AtMTM1* and *AtMTM2* expression level, we did qRT-PCR assay to compare their level in leaves between normal condition and stress condition. Our result showed the *AtMTM1* was indeed induced by osmosis stress, but not as much as previously reported (Ndamukong, Jones et al. 2010). Interestingly, the *AtMTM2* presented a slight decrease pattern. This decrease indicated the role of AtMTM2 might be greatly different from AtMTM1, at least in leaves. Since AtMTM2 showed a higher expression in roots, its expression might be enhanced there. However, we are lack of data to answer this question. Therefore, further studies should investigated whether or not AtMTM2 expression is elevated in roots after stress, and also in flowers and siliques. Because AtMTM1 expression level didn't increase significantly,

another possible mechanism might exist in regulating AtMTM1 enzymatic activity involved in PI5P metabolism. Or it is possible that the expression is specifically sharply increased in some organs of leaves, such as hydathodes. Thus, when consider the leaves as a whole could hardly give useful information. Based on these possibilities, more data is required to show the specific change of each expression level under osmosis stress.

### **Cytoplasmic AtMTM1 but nuclear AtMTM2?**

In this thesis, we failed to provide convincing evidence of AtMTM2 localization. Our data indicated AtMTM2 was lack of specificity. However, this could be due to the single mutation. Therefore, this localization analysis should be repeated again with the intact native sequence.

Though lack of specificity, it doesn't exclude the possibility that AtMTM2 could enter nucleus. Previous studies found very few myotubularins in the nucleus. Thus, there is a large blank left on regulatory function of myotubularins in nucleus. AtMTM2 might play direct role in gene expression in the nucleus. In contrast, AtMTM1 only locates in the cytoplasm and along membrane, and doesn't enter nucleus. The interesting difference from AtMTM2 is AtMTM1 exists as small patches in the cytoplasm, which indicates that AtMTM1 functions as a large complex. Future work should find out which proteins are included in this complex and their affect on the AtMTM1 activity.

By co-expression of AtMTM1 and AtMTM2 in the same cell, we had a chance to find out if they interact with each other. Because they didn't show any colocalization patterns, they could hardly interact or even form heterodimers. Thus, the hypothesis that dimerization may regulate the AtMTM1 substrate specificity cannot be accepted.

## Phenotypic characterization of mutant plants

Isolation of stable and well characterized mutant lines is crucial for the efforts in this research to study functional and regulatory effects resulting from *AtMTM1*, *AtMTM2* and both of them loss of function and to address further questions. We hope to provide an in-depth view on the physiological influence of the two closely related factors in *Arabidopsis*.

During the vegetative growth, there were no defects observed in all mutants. The difference between mutants relies on their response to drought stress. ***atmtm1-1*** presented a phenotype that it flowered earlier and taller than wild type. And after rehydration, there were more mutants survived than wild type. These data suggests the importance of AtMTM1 in drought tolerance and resistance. However, because of the lack in documenting the flower phenotype in normal condition compared with Col 0, another interpretation is still possible: the earlier and taller flower is not due to drought stress. Instead, the mutant might show the same phenotype in normal condition simply due to the loss of functional AtMTM1. In addition, the sample size was only 10, which is too small to be statistically convincing. Therefore, future studies need to specify AtMTM1 physiological function in drought condition and prove it statistically.

The other *AtMTM1* disrupted mutant didn't share the same phenotype with ***atmtm1-1***. This is probably because there were still truncated mRNAs of AtMTM1 functioning in the mutant. Whether a truncated AtMTM1 still maintains the complete function is unclear. But the difference between ***atmtm1-1*** and ***atmtm1-2*** suggests the amount of functional AtMTM1 also matters in stress tolerance.

By comparison, ***atmtm2*** did not show any derived character from wild type, even in drought condition. This observation indicates the AtMTM2 is not involved in the regulatory response to osmosis stress, although it is in the nucleus. So, the

question that what is the function of AtMTM2 requires further studies to answer.

## CONCLUSION

We investigated the expression patterns of AtMTM1 and AtMTM2. We found both of them are ubiquitously present in roots, leaves, flowers and siliques, and they are more abundant in new synthesized tissues and actively developing cells. Specifically, AtMTM2 showed a stronger expression in roots and trichomes while AtMTM1 increased visibly in hydathodes after dehydration. Our qRT-PCR analysis confirmed the increase of *AtMTM1* in leaves under stress.

We compared the sub-cellular localization of AtMTM1 and AtMTM2. While AtMTM1 exists in the cytoplasm and along membrane as small patches, similarly to most myotubularins; AtMTM2 doesn't show any specificity with a mutation in the 250<sup>th</sup> amino acid. When coexpress them together in the same cell, they failed to show a co-localization pattern. We then conclude that AtMTM1 needs to be integrated into a complex to complete its function, whereas AtMTM2 may have a role in regulation of gene expression in the nucleus. Importantly, they cannot form heterodimers at current experimental conditions.

We isolated homozygous mutants of *AtMTM1*, *AtMTM2* and both of them. All of the mutants could grow normally compared with Col 0 in water condition. But complete loss of functional AtMTM1 would enhance the drought tolerance ability. However, *AtMTM2* didn't show any deviation even after drought stress, which indicates its function is probably not involved in the regulation of the response to osmosis stress.

## REFERENCED LITERATURE

- Alvarez-Venegas, R. (2006). "The *Arabidopsis* homolog of trithorax, ATX1, binds phosphatidylinositol 5-phosphate, and the two regulate a common set of target genes." *Proceedings of the National Academy of Sciences* **103**(15): 6049-6054.
- Azzedine, H., A. Bolino, et al. (2003). "Mutations in MTMR13, a new pseudophosphatase homologue of MTMR2 and Sbf1, in two families with an autosomal recessive demyelinating form of Charcot-Marie-Tooth disease associated with early-onset glaucoma." *Am J Hum Genet* **72**(5): 1141-1153.
- Begley, M. and J. Dixon (2005). "The structure and regulation of myotubularin phosphatases." *Current Opinion in Structural Biology* **15**(6): 614-620.
- Berger, P., I. Berger, et al. (2006). "Multi-level regulation of myotubularin-related protein-2 phosphatase activity by myotubularin-related protein-13/set-binding factor-2." *Hum Mol Genet* **15**(4): 569-579.
- Bolino, A., A. Bolis, et al. (2004). "Disruption of Mtnmr2 produces CMT4B1-like neuropathy with myelin outfolding and impaired spermatogenesis." *J Cell Biol* **167**(4): 711-721.
- Bolino, A., M. Muglia, et al. (2000). "Charcot-Marie-Tooth type 4B is caused by mutations in the gene encoding myotubularin-related protein-2." *Nat Genet* **25**(1): 17-19.
- Bua, D. J. and O. Binda (2009). "The return of the INGs, histone mark sensors and phospholipid signaling effectors." *Curr Drug Targets* **10**(5): 418-431.
- Bunce, M. W., M. L. Gonzales, et al. (2006). "Stress-ING out: phosphoinositides mediate the cellular stress response." *Sci STKE* **2006**(360): pe46.
- Cao, C., J. Laporte, et al. (2007). "Myotubularin lipid phosphatase binds the hVPS15/hVPS34 lipid kinase complex on endosomes." *Traffic* **8**(8): 1052-1067.
- Clague, M. J. and Ó. Lorenzo (2005). "The Myotubularin Family of Lipid Phosphatases." *Traffic* **6**(12): 1063-1069.
- Clarke, J. H. (2003). "Lipid signalling: picking out the PIPs." *Curr Biol* **13**(20): R815-817.

- De Matteis, M. A. and A. Godi (2004). "PI-loting membrane traffic." Nat Cell Biol **6**(6): 487-492.
- Ding, Y., H. Lapko, et al. (2009). "The *Arabidopsis* chromatin modifier ATX1, the myotubularin-like AtMTM and the response to drought." Plant Signal Behav **4**(11): 1049-1058.
- Firestein, R., P. L. Nagy, et al. (2002). "Male infertility, impaired spermatogenesis, and azoospermia in mice deficient for the pseudophosphatase Sbf1." J Clin Invest **109**(9): 1165-1172.
- Gaullier, J. M., A. Simonsen, et al. (1998). "FYVE fingers bind PtdIns(3)P." Nature **394**(6692): 432-433.
- Godi, A., A. Di Campli, et al. (2004). "FAPPs control Golgi-to-cell-surface membrane traffic by binding to ARF and PtdIns(4)P." Nat Cell Biol **6**(5): 393-404.
- Gozani, O., S. J. Field, et al. (2005). "Modification of protein sub-nuclear localization by synthetic phosphoinositides: evidence for nuclear phosphoinositide signaling mechanisms." Adv Enzyme Regul **45**: 171-185.
- Gozani, O., P. Karuman, et al. (2003). "The PHD finger of the chromatin-associated protein ING2 functions as a nuclear phosphoinositide receptor." Cell **114**(1): 99-111.
- Hirst, J., A. Motley, et al. (2003). "EpsinR: an ENTH domain-containing protein that interacts with AP-1." Mol Biol Cell **14**(2): 625-641.
- Jones and D. (2004). "Linking lipids to chromatin." Current Opinion in Genetics & Development **14**(2): 196-202.
- Jung, J. Y., Y. W. Kim, et al. (2002). "Phosphatidylinositol 3- and 4-phosphate are required for normal stomatal movements." Plant Cell **14**(10): 2399-2412.
- Kim, S. A., P. O. Vacratsis, et al. (2003). "Regulation of myotubularin-related (MTMR)2 phosphatidylinositol phosphatase by MTMR5, a catalytically inactive phosphatase."

Proc Natl Acad Sci U S A **100**(8): 4492-4497.

Laporte, J., L. J. Hu, et al. (1996). "A gene mutated in X-linked myotubular myopathy defines a new putative tyrosine phosphatase family conserved in yeast." Nat Genet **13**(2): 175-182.

Lecompte, O., O. Poch, et al. (2008). "PtdIns5P regulation through evolution: roles in membrane trafficking?" Trends in Biochemical Sciences **33**(10): 453-460.

Levine, T. P. and S. Munro (2002). "Targeting of Golgi-specific pleckstrin homology domains involves both PtdIns 4-kinase-dependent and -independent components." Curr Biol **12**(9): 695-704.

Lorenzo, O., S. Urbe, et al. (2006). "Systematic analysis of myotubularins: heteromeric interactions, subcellular localisation and endosome related functions." J Cell Sci **119**(Pt 14): 2953-2959.

Meijer, H. J., C. P. Berrie, et al. (2001). "Identification of a new polyphosphoinositide in plants, phosphatidylinositol 5-monophosphate (PtdIns5P), and its accumulation upon osmotic stress." Biochem J **360**(Pt 2): 491-498.

Morris, J. B., K. A. Hinchliffe, et al. (2000). "Thrombin stimulation of platelets causes an increase in phosphatidylinositol 5-phosphate revealed by mass assay." FEBS Lett **475**(1): 57-60.

Ndamukong, I., D. R. Jones, et al. (2010). "Phosphatidylinositol 5-phosphate links dehydration stress to the activity of *ARABIDOPSIS* TRITHORAX-LIKE factor ATX1." PLoS One **5**(10): e13396.

Niebuhr, K., S. Giuriato, et al. (2002). "Conversion of PtdIns(4,5)P<sub>2</sub> into PtdIns(5)P by the *S.flexneri* effector IpgD reorganizes host cell morphology." EMBO J **21**(19): 5069-5078.

Pendaries, C., H. Tronchere, et al. (2006). "PtdIns5P activates the host cell PI3-kinase/Akt

- pathway during *Shigella flexneri* infection." *EMBO J* **25**(5): 1024-1034.
- Pendaries, C., H. Tronchere, et al. (2005). "Emerging roles of phosphatidylinositol monophosphates in cellular signaling and trafficking." *Advances in Enzyme Regulation* **45**(1): 201-214.
- Ponting, C. P. (1996). "Novel domains in NADPH oxidase subunits, sorting nexins, and PtdIns 3-kinases: binding partners of SH3 domains?" *Protein Sci* **5**(11): 2353-2357.
- Rameh, L. E., K. F. Tolias, et al. (1997). "A new pathway for synthesis of phosphatidylinositol-4,5-bisphosphate." *Nature* **390**(6656): 192-196.
- Robinson, F. L. and J. E. Dixon (2005). "The phosphoinositide-3-phosphatase MTMR2 associates with MTMR13, a membrane-associated pseudophosphatase also mutated in type 4B Charcot-Marie-Tooth disease." *J Biol Chem* **280**(36): 31699-31707.
- Sbrissa, D., O. C. Ikonomov, et al. (2002). "Phosphatidylinositol 5-phosphate biosynthesis is linked to PIKfyve and is involved in osmotic response pathway in mammalian cells." *J Biol Chem* **277**(49): 47276-47284.
- Sbrissa, D., O. C. Ikonomov, et al. (2004). "Role for a novel signaling intermediate, phosphatidylinositol 5-phosphate, in insulin-regulated F-actin stress fiber breakdown and GLUT4 translocation." *Endocrinology* **145**(11): 4853-4865.
- Shisheva, A. (2001). "PIKfyve: the road to PtdIns 5-P and PtdIns 3,5-P(2)." *Cell Biol Int* **25**(12): 1201-1206.
- Tolias, K. F. and L. C. Cantley (1999). "Pathways for phosphoinositide synthesis." *Chem Phys Lipids* **98**(1-2): 69-77.
- Tronchere, H., A. Buj-Bello, et al. (2003). "Implication of phosphoinositide phosphatases in genetic diseases: the case of myotubularin." *Cell Mol Life Sci* **60**(10): 2084-2099.
- Tronchere, H., J. Laporte, et al. (2004). "Production of phosphatidylinositol 5-phosphate by the phosphoinositide 3-phosphatase myotubularin in mammalian cells." *J Biol Chem*

**279**(8): 7304-7312.

Walker, D. M., S. Urbe, et al. (2001). "Characterization of MTMR3. an inositol lipid 3-phosphatase with novel substrate specificity." Curr Biol **11**(20): 1600-1605.

Wang, Y. J., J. Wang, et al. (2003). "Phosphatidylinositol 4 phosphate regulates targeting of clathrin adaptor AP-1 complexes to the Golgi." Cell **114**(3): 299-310.

Wu, B., K. Kitagawa, et al. (2002). "Phosphatidylinositol and PI-4-monophosphate recover amyloid beta protein-induced inhibition of Cl<sup>-</sup> -ATPase activity." Life Sci **72**(4-5): 455-463.